UNIVERSITY OF CALIFORNIA
RIVERSIDE

Gray Matter Diffusion Imaging Captures Individual and Age Group Differences in Microstructure and Memory Performance

A Dissertation submitted in partial satisfaction
of the requirements for the degree of

Doctor of Philosophy

in

Neuroscience

by

Anu Venkatesh

June 2021

Dissertation Committee:
Dr. Ilana J. Bennett, Chairperson
Dr. Chandra A. Reynolds
Dr. Weiwei Zhang

The Dissertation of Anu Venkatesh is approved:

_____

_____

_____

Committee Chairperson

University of California, Riverside

Acknowledgements

Thank you to my advisor, Lani, for her patient guidance throughout this process. I have learned so much from you and will carry those standards with me throughout my career. Thank you also to the research assistants, lab mates, and UCR staff for all your help and support throughout the last five years.

This work was supported by the Science, Mathematics and Research for Transformation (SMART) program from the U.S. Department of Defense.

Dedication

To my mother, Malathi, and my late maternal grandmothers, Vimala and Srividhya. My access to an education was built on your sacrifices. You are my source of inspiration and strength. Thank you.

ABSTRACT OF THE DISSERTATION

Gray Matter Diffusion Imaging Captures Individual and Age Group Differences in Microstructure and Memory Performance

by

Anu Venkatesh

Doctor of Philosophy, Graduate Program in Neuroscience
University of California, Riverside, June 2021
Dr. Ilana J. Bennett, Chairperson

One of the central goals of neuroscience is to understand how the brain impacts behavior, this understanding can help explain why some individuals undergo normal age-related memory decline while others develop dementia. To this end, the current body of work utilized multi-compartment diffusion imaging to characterize brain wide differences in gray matter microstructure and examined relationships to memory performance, using young and older adults. This approach was sensitive to restricted, hindered, and free diffusion compartments, which are thought to reflect intra- and extra-cellular diffusion, and cerebral spinal fluid, respectively. Initial results with 51 participants (chapter 1) in the hippocampus revealed that multi-compartment diffusion measures outperformed traditional single-tensor measures to capture differences in age and memory performance, likely to improved sensitivity to gray matter microstructure including differences in the free water compartment. A follow up with 146 participants (chapter 2) revealed that the previously observed effects extended to gray matter regions beyond the hippocampus.

Frontal lobe free diffusion was the top ranked predictor of age and was negatively, strengthening the association between of free water and age. Within hippocampus, relationships to memory performance revealed that hindered and restricted diffusion were selective to different facets of memory performance; negative associations were observed between hindered diffusion and mnemonic discrimination, and between restricted diffusion and recall performance. This negative association with recall, in addition to an age-related increase in restricted diffusion suggested that diffusion measures may be sensitive to gray matter gliosis. The last experiment with a subset of 63 participants from the previous chapter (chapter 3) supported this theoretical framework by demonstrating that diffusion measures were positively associated with iron content, consistent with the model of iron-related inflammation and gliosis established in animals. The shared variance between iron and restricted diffusion also helped explain differences in recall memory performance, since higher restricted diffusion was associated with poorer memory performance. Overall, this body of work moves the field of neuroscience forward by demonstrating that gray matter microstructure differs between young and older adults in specific ways and identifies gliosis as a contributor to differences in human memory.

Table of Contents

List of Figures

Chapter 1

Chapter 2

Chapter 3

List of Tables

Chapter 1

Chapter 2

Chapter 3

General Introduction

Due to increasing life expectancy and decreasing fertility rate, the global population is aging and facing challenges such as age-related cognitive decline (Lutz, Sanderson, & Scherbov, 2008). Cognitive aging can cause both normal and pathological (e.g., dementia) declines in cognition over the lifespan (Harada, Natelson Love, & Triebel, 2013), with memory decline in particular having a profound negative effect on individuals' quality of life. The trajectory of cognitive aging over the lifespan can be improved by better understanding individual and age-related differences in the brain and relationships to memory performance. To this end, the current body of work utilizes multi-compartment diffusion imaging to characterize age-related differences in gray matter microstructure and identifies how specific neurobiological variables (e.g., glia, neurites, cerebral spinal fluid; CSF) may contribute to differences in memory performance. Using gray matter diffusion imaging in young and older adults, the results presented across three chapters will demonstrate (1) significant age-related microstructural differences in the hippocampus, a region critical to memory, (2) brain wide differences in gray matter microstructure that extend existing hypotheses of cognitive aging, and (3) *in vivo* validation of a model of memory decline involving iron-accumulation and gliosis.

The first chapter focuses on diffusion imaging in the hippocampus, a region that is critical to memory and known to be affected by aging (Lister & Barnes, 2009). This chapter compares newer diffusion approaches like Neurite Orientation Dispersion and Density Imaging (NODDI; Zhang, Schneider, Wheeler-Kingshott, & Alexander, 2012),

to the traditional, diffusion tensor imaging (DTI) to establish the improved sensitivity of the former compared to the latter. An advantage of NODDI is that the complexity of gray matter can be more accurately represented, compared to DTI which summarizes all diffusion within gray matter into general estimates of anisotropy and rate of diffusion. Gray matter is more complex than that, so understanding the contributions of intracellular, extracellular and CSF compartments to age group differences is important for identifying specific biological variables that are affected by age. Subdividing hippocampal diffusion into these compartments of restricted, hindered and free diffusion will improve sensitivity to age group differences while reducing the potential for partial-volume effects (Metzler-Baddeley, O'Sullivan, Bells, Pasternak, & Jones, 2012; Pasternak, Sochen, Gur, Intrator, & Assaf, 2009), which refers to a voxel containing multiple tissue types and free water. Previous studies (Chad, Pasternak, Salat, & Chen, 2018a; Sasson, Doniger, Pasternak, Tarrasch, & Assaf, 2012) have reported that white matter free water was significantly associated with age and cognition, which suggests that a separate measure of free diffusion could itself be a valuable marker of aging. This led to the question of whether these patterns extend to gray matter as well as to regions beyond the hippocampus.

Chapter two extends the use of NODDI to cortical lobes and striatal regions (in addition to hippocampus) to examine brain wide age group differences in gray matter microstructure. This approach allowed testing of the free water relationship with age as well as the frontal lobe hypothesis (West, 1996), which suggests that the effect of age is more severe on anterior portions of the brain compared to posterior portions. In addition,

multiple memory measures (recall, recognition and mnemonic discrimination) can be used to identify the specific relationships between gray matter microstructure and facets of memory. For example, while traditional recognition memory may be associated with overall cell density, as measured by restricted diffusion, mnemonic discrimination (the ability to discriminate between similar events) is thought to rely on pattern separation supported by granule cell dendrites (Chavlis, Petrantonakis, & Poirazi, 2017), whose cell complexity can be measured by hindered diffusion. Therefore, the overall aim of this chapter is to distinguish between the specific contributions of restricted, hindered, and free diffusion, to regional gray matter age group differences and memory performance.

Chapter three leverages the findings from the previous two chapters to corroborate an animal model of iron-related memory decline using multi-compartment diffusion imaging in conjunction with quantitative relaxometry in young and older adults. Previous *in vivo* (Thomsen et al., 2015; You et al., 2017) studies in animal models have directly linked iron-related inflammation to reactive gliosis and subsequent memory decline (Schröder, Figueiredo, & De Lima, 2013b; M. Weber et al., 2015). Consistent with the Free-Radical-Induced Energetic and Neural Decline in Senescence (FRIENDS; Raz & Daugherty, 2018) model, this chapter examines the relationships between iron, gliosis and memory performance using MRI techniques like quantitative relaxometry along with diffusion imaging. Based on the pattern of results from chapters two and three and previous studies in animals (Debacker, Djemai, Ciobanu, Tsurugizawa, & Bihan, 2020; Yi et al., 2019) it was hypothesized that restricted, hindered and free diffusion were sensitive to different phenotypes of gliosis such as activation (e.g. astrocyte swelling;

Norenberg, 1994; Pekny & Nilsson, 2005; Singh, Trivedi, Devi, Tripathi, & Khushu, 2016), proliferation (e.g. microglia recruitment; Yi et al., 2019) and dysfunction (e.g. increased blood-brain permeability; Oakley & Tharakan, 2014; Simon & Iliff, 2016). Thus, it was predicted that relationships between diffusion measures, iron content and memory performance would be consistent with iron-gliosis patterns observed in animal models. The aim of this chapter is to link the previous diffusion findings to an animal model of cognitive aging and test whether relationships between diffusion and iron content are consistent with those predicted by the iron-gliosis model, using noninvasive MRI techniques.

Overall, this body of work improves understanding of differences in human gray matter microstructure, as well as relationships to age and memory performance. In the future, these results may inform the use of NODDI measures as biomarkers of age and memory decline to distinguish normal cognitive aging with pathological trajectories. For now, these data move the field of neuroscience forward by validating animal models of aging in humans and demonstrate that MRI techniques have great utility in investigating brain-behavior relationships.

References

Chad, J. A., Pasternak, O., Salat, D. H., & Chen, J. J. (2018). Re-examining age-related differences in white matter microstructure with free-water corrected diffusion tensor imaging. *Neurobiology of Aging*, *71*, 161–170. https://doi.org/10.1016/J.NEUROBIOLAGING.2018.07.018

Chavlis, S., Petrantonakis, P. C., & Poirazi, P. (2017). Dendrites of dentate gyrus granule cells contribute to pattern separation by controlling sparsity. *Hippocampus*, *27*(1), 89–110. https://doi.org/10.1002/hipo.22675

Debacker, C., Djemai, B., Ciobanu, L., Tsurugizawa, T., & Bihan, D. Le. (2020). Diffusion MRI reveals in vivo and non-invasively changes in astrocyte function induced by an aquaporin-4 inhibitor. *PLoS ONE*, *15*(5). https://doi.org/10.1371/journal.pone.0229702

Harada, C. N., Natelson Love, M. C., & Triebel, K. L. (2013). Normal cognitive aging. *Clinics in Geriatric Medicine*, *29*(4), 737–752. https://doi.org/10.1016/j.cger.2013.07.002

Lister, J. P., & Barnes, C. A. (2009). Neurobiological changes in the hippocampus during normative aging. *Archives of Neurology*, *66*(7), 829–833. https://doi.org/10.1001/archneurol.2009.125

Lutz, W., Sanderson, W., & Scherbov, S. (2008). The coming acceleration of global population ageing. *Nature*, *451*(7179), 716–719. https://doi.org/10.1038/nature06516

Metzler-Baddeley, C., O'Sullivan, M. J., Bells, S., Pasternak, O., & Jones, D. K. (2012). How and how not to correct for CSF-contamination in diffusion MRI. *NeuroImage*, *59*(2), 1394–1403. https://doi.org/10.1016/J.NEUROIMAGE.2011.08.043

Norenberg, M. D. (1994). Astrocyte Responses to CNS Injury. *Journal of Neuropathology and Experimental Neurology*, *53*(3), 213–220. https://doi.org/10.1097/00005072-199405000-00001

Oakley, R., & Tharakan, B. (2014). Vascular Hyperpermeability and Aging. *Aging and Disease*, *5*(2), 114–125. https://doi.org/10.14336/AD.2014.0500114

Pasternak, O., Sochen, N., Gur, Y., Intrator, N., & Assaf, Y. (2009). Free water elimination and mapping from diffusion MRI. *Magnetic Resonance in Medicine*, *62*(3), 717–730. https://doi.org/10.1002/mrm.22055

Pekny, M., & Nilsson, M. (2005). Astrocyte activation and reactive gliosis. *Glia*, *50*(4), 427–434. https://doi.org/10.1002/glia.20207

Sasson, E., Doniger, G. M., Pasternak, O., Tarrasch, R., & Assaf, Y. (2012). Structural correlates of cognitive domains in normal aging with diffusion tensor imaging. *Brain Structure and Function*, *217*(2), 503–515. https://doi.org/10.1007/s00429-011-0344-7

Schröder, N., Figueiredo, L. S., & De Lima, M. N. M. (2013a). Role of brain iron accumulation in cognitive dysfunction: Evidence from animal models and human studies. *Journal of Alzheimer's Disease*, *34*(4), 797–812. https://doi.org/10.3233/JAD-121996

Schröder, N., Figueiredo, L. S., & De Lima, M. N. M. (2013b). Role of brain iron accumulation in cognitive dysfunction: Evidence from animal models and human studies. *Journal of Alzheimer's Disease*. IOS Press. https://doi.org/10.3233/JAD-121996

Simon, M. J., & Iliff, J. J. (2016, March 1). Regulation of cerebrospinal fluid (CSF) flow in neurodegenerative, neurovascular and neuroinflammatory disease. *Biochimica et Biophysica Acta - Molecular Basis of Disease*. Elsevier. https://doi.org/10.1016/j.bbadis.2015.10.014

Singh, K., Trivedi, R., Devi, M. M., Tripathi, R. P., & Khushu, S. (2016). Longitudinal changes in the DTI measures, anti-GFAP expression and levels of serum inflammatory cytokines following mild traumatic brain injury ☆. *Experimental Neurology*, *275*, 427–435. https://doi.org/10.1016/j.expneurol.2015.07.016

Thomsen, M. S., Andersen, M. V., Christoffersen, P. R., Jensen, M. D., Lichota, J., & Moos, T. (2015). Neurodegeneration with inflammation is accompanied by accumulation of iron and ferritin in microglia and neurons. *Neurobiology of Disease*, *81*, 108–118. https://doi.org/10.1016/j.nbd.2015.03.013

Weber, M., Wu, T., Hanson, J. E., Alam, N. M., Solanoy, H., Ngu, H., … Levie, K. S. (2015). Cognitive deficits, changes in synaptic function, and brain pathology in a mouse model of normal aging. *ENeuro*, *2*(5), 47–62. https://doi.org/10.1523/ENEURO.0047-15.2015

West, R. L. (1996). An application of prefrontal cortex function theory to cognitive aging. *Psychological Bulletin*, *120*(2), 272–292. https://doi.org/10.1037/0033-2909.120.2.272

Yi, S. Y., Barnett, B. R., Torres-Velázquez, M., Zhang, Y., Hurley, S. A., Rowley, P. A., … Yu, J. P. J. (2019). Detecting microglial density with quantitative multi-compartment diffusion MRI. *Frontiers in Neuroscience*. https://doi.org/10.3389/fnins.2019.00081

You, L. H., Yan, C. Z., Zheng, B. J., Ci, Y. Z., Chang, S. Y., Yu, P., … Chang, Y. Z. (2017). Astrocyte hepcidin is a key factor in LPS-induced neuronal apoptosis. *Cell Death & Disease*, *8*(3), e2676. https://doi.org/10.1038/cddis.2017.93

Zhang, H., Schneider, T., Wheeler-Kingshott, C. A., & Alexander, D. C. (2012). NODDI: Practical in vivo neurite orientation dispersion and density imaging of the human brain. *NeuroImage*, *61*(4), 1000–1016. https://doi.org/10.1016/j.neuroimage.2012.03.072

Chapter 1: Age- and Memory- Related Differences in Hippocampal Gray Matter Integrity Are Better Captured by NODDI Compared to Single-Tensor Diffusion Imaging

Abstract

Single-tensor diffusion imaging (DTI) has traditionally been used to assess integrity of white matter. For example, we previously showed that integrity of limbic white matter tracts declines in healthy aging and relates to episodic memory performance. However, multi-compartment diffusion models may be more informative about microstructural properties of gray matter. The current study examined hippocampal gray matter integrity using both single-tensor and multi-compartment (neurite orientation dispersion and density imaging, NODDI) diffusion imaging. Younger (20-38 years) and older (59-84 years) adults also completed the Mnemonic Similarity Task to measure mnemonic discrimination performance. Results revealed age-related declines in both single-tensor (lower fractional anisotropy, higher mean diffusivity) and multi-compartment (higher restricted, hindered and free diffusion) measures of hippocampal gray matter integrity. As expected, NODDI measures (hindered and free diffusion) captured more age-related variance than DTI measures. Moreover, mnemonic discrimination of highly similar lure items in memory was related to hippocampal gray matter integrity in younger but not older adults. These findings support the notion that age-related differences in gray matter integrity are better captured by multi-compartment versus single-tensor diffusion models and show that the relationship between mnemonic discrimination and hippocampal gray matter integrity is moderated by age.

Introduction

The hippocampus, which is critical for episodic memory, is known to be affected in healthy aging (Lister & Barnes, 2009; Scahill et al., 2003), even in absence of dementia (Park & Reuter-Lorenz, 2009). Structural neuroimaging studies, for example, have shown age-related declines in hippocampal macrostructure, with decreased volume seen in whole hippocampus in older adults relative to younger adults (Doxey & Kirwan, 2015; Raz et al., 2005). In the last decade, diffusion imaging has allowed for in vivo examinations of neural microstructure, with numerous studies reporting age-related differences in the integrity of white matter (de Lange et al., 2016; Gunning-Dixon, Brickman, Cheng, & Alexopoulos, 2009; Madden et al., 2012), including white matter tracts projecting to and from the hippocampus (e.g. fornix, cingulum; Bennett, Huffman, & Stark, 2015; Bennett & Stark, 2016). However, few studies have assessed whether diffusion imaging may also be a promising tool for evaluating microstructural properties of hippocampal gray matter in aging, especially as it relates to episodic memory performance.

Diffusion imaging data is traditionally modeled as a single tensor per voxel that summarizes the rate of molecular water diffusion along three axes (diffusion tensor imaging, DTI; Beaulieu, 2002; Hassan et al., 2014). This single-tensor DTI approach yields metrics, such as the degree of restricted diffusion (fractional anisotropy, FA) and average rate of diffusion (mean diffusivity, MD), from which the integrity of underlying tissue can be inferred. In white matter, for example, higher FA and lower MD would be seen in regions with highly aligned, densely packed, and tightly myelinated axonal fibers.

Across the lifespan, decreases in FA and increases in MD (Bennett et al., 2015; Gunning-Dixon et al., 2009; Madden et al., 2012) are interpreted as declines in white matter integrity (e.g., age-related demyelination). In gray matter, however, the underlying tissue is relatively less organized (e.g. dendrites, cell bodies, glia), resulting in lower FA and higher MD than white matter. Owing to this microstructural complexity, the single-tensor approach alone may not be suited for accurately modeling diffusion in gray matter.

A potentially more accurate way to assess microstructural properties of gray matter is with multi-compartment diffusion approaches that separately model different sources (compartments or volume fractions) of the total diffusion signal (Fukutomi et al., 2018a; Kaden, Kelm, Carson, Does, & Alexander, 2016; Rae et al., 2017). Neurite Orientation Dispersion and Density Imaging (NODDI; Zhang, Schneider, Wheeler-Kingshott, & Alexander, 2012), for example, models restricted diffusion (also known as neurite density index; NDI) as a set of sticks, hindered diffusion (also known as orientation dispersion index; ODI) as the dispersion of the sticks, and unrestricted diffusion (also known as isotropic fraction; fISO) as an isotropic sphere (Fukutomi et al., 2018a; Rae et al., 2017; H. Zhang et al., 2012). Differences in these metrics may result from microstructural properties that affect intracellular, extracellular, and free sources of diffusion (e.g. age-related increases in cell swelling, loss of spines or synaptic remodeling, and vascular permeability; Clarke et al., 2018; Dickstein et al 2013, Szebenyi et al., 2005; Elahy et al., 2015, respectively). An additional advantage of this multi-compartment approach is that the free diffusion metric can be used to account for free

diffusion contamination in remaining integrity metrics, which is prevalent in the aging brain (Chad, Pasternak, Salat, & Chen, 2018b; Metzler-Baddeley et al., 2012; Rathi et al., 2014).

Multiple diffusion imaging studies have examined the effect of aging on gray matter integrity using either single-tensor (Bhagat and Beaulieu, 2004, Càmara et al., 2007; Carlesimo et al., 2010; Cherubini et al., 2009; Den Heijer et al., 2012; Pereira et al., 2014; Pfefferbaum et al., 2010; Rathi et al., 2014; Salminen et al., 2016; Sasson et al., 2012) or multi-compartment (Fukutomi et al., 2018; Kaden et al., 2016; Nazeri et al., 2017) approaches, but only a handful have assessed aging of hippocampal gray matter integrity. Using the single-tensor approach, studies have reported age-related increases in hippocampal MD (Carlesimo et al., 2010, Pereira et al., 2014), no change (Cherubini et al., 2009) or mixed results depending on the region profiled (Pfefferbaum et al. 2010, Salminen et al., 2016). After excluding free diffusion (e.g., using cerebrospinal fluid [CSF]-suppression diffusion imaging or region of interest [ROI] based segmentation), DTI studies have found both age-related increases in hippocampal FA (Rathi et al., 2014) and age-related decrease in anterior hippocampal relative anisotropy (Càmara et al., 2007). Using the NODDI multi-compartment approach, at least one study demonstrated that hindered diffusion within bilateral hippocampus increased with age in adults across a lifespan sample (age 21-84; Nazeri et al., 2015). However, because none of these studies directly compared single-tensor and multi-compartment models, it remains unknown whether these age differences in DTI and NODDI metrics are capturing similar microstructural mechanisms within hippocampus. The functional relevance of

hippocampal gray matter integrity in non-demented older adults also remains understudied. Previous single-tensor DTI studies have reported that hippocampal MD was associated with impaired episodic memory assessed by a list learning (Den Heijer et al., 2012) and visuospatial task (Carlesimo et al., 2010). An important component of successful episodic memory is mnemonic discrimination, the ability to discriminate between highly similar events in memory. Using a modified recognition task, the Mnemonic Similarity Task (MST; Stark et al., 2013, Kirwan & Stark, 2007), our group has previously shown that mnemonic discrimination declines in healthy aging (Stark, Yassa, Lacy, & Stark, 2013a) and that worse discrimination performance is related to lower integrity of white matter tracts projecting to (perforant path; Bennett & Stark, 2016; Yassa, Muftuler, & Stark, 2010) and emanating from (fornix; Bennett et al, 2015) the hippocampus in adults across the lifespan. However, these effects have not been assessed for hippocampal gray matter integrity using either single-tensor or multi-compartment diffusion metrics.

Building on this work, the current study examined hippocampal gray matter integrity using both single-tensor (DTI) and multi-compartment (NODDI) diffusion modeling of the same diffusion data in younger and older adults (20-38 and 59-84 years, respectively) who also completed the MST. Our primary aim was to assess age-related differences in hippocampal gray matter integrity and in particular whether the multi-compartment diffusion approach was more sensitive to hippocampal aging than the single-tensor approach. To assess whether free diffusion influences traditional integrity metrics (e.g., from partial volume effects with adjacent CSF), the effect of age on single-

tensor integrity measures were examined before (unthresholded DTI) and after (thresholded DTI) accounting for the NODDI free diffusion compartment. Our secondary aim was to determine whether hippocampal gray matter integrity relates to mnemonic discrimination performance.

Materials and Methods

Participants

Fifty-one adults were recruited from the University of California, Irvine and surrounding Orange County neighborhoods. One older participant was excluded for poor general cognition (Mini-Mental State Exam [MMSE] < 28; Folstein et al. 1975) and one young participant was excluded for neuroimaging segmentation errors. The final sample included 24 younger (20-38 years, 27.6 ± 5.1 years, 12 females) and 25 older (59-84 years, 69.9 ± 5.31 years, 14 females) adults. The final sample of 24 younger and 25 older adults were used for all analyses except the behavioral analysis as detailed below.

All individuals provided informed consent prior to participation in this study. The University of California, Irvine Institutional Review Board (IRB) approved the experimental procedures and participants were compensated for their time.

Neuropsychological Battery

To characterize their cognitive profiles, participants underwent a battery of neuropsychological tests including the MMSE to assess general cognition; Rey Auditory Verbal Learning Test (RAVLT) to assess recall and recognition (Rey 1941); Geriatric Depression Scale (GDS) and Beck Depression Index (BDI) to assess depression status (Yesavage et al. 1982, Beck, et al. 1961); Trails A and B, Stroop test and Letter Number

Sequencing to assess executive functioning (Reitan and Wolfson 1985, Stroop 1935, and Wechsler 1997a); Digit Span to assess working memory (Wechsler 1997a); and Physical Activity Scale for the Elderly (PASE) to assess overall activity level (Washburn et al. 1993). These data are presented in Table 1.

Mnemonic Similarity Task

Mnemonic discrimination was assessed using the Mnemonic Similarity Task (MST; see Stark et al 2013 for additional details). In separate incidental study and test phases, participants viewed a series of common objects (e.g. rubber duck, piano) in color on a white background. During the study phase, participants judged whether each object belongs "indoors" or "outdoors" via button press. During the test phase, participants judged whether objects were repeated from the study phase (target), similar to objects from the study phase (lure), or completely new (novel) using "old", "similar" or "new" responses, respectively. Mnemonic discrimination was assessed using the Lure Discrimination Index (LDI), calculated as the probability of correctly judging lures as "similar" after accounting for any bias in using the "similar" response: $LDI = p(\text{"similar"}|lure) - p(\text{"similar"}|novel)$. Additionally, Recognition was calculated as the probability of correctly judging targets as "old" after accounting for any bias in using the "old" response: Recognition = $p(\text{"old"}|target) - p(\text{"old"}|novel)$. Some participants were excluded from the MST analysis if they had a large number of omitted responses (> 80% of trials; 4 younger adults) or poor Recognition (> 2 SD from the overall mean; 3 younger, 1 older adult).

Neuroimaging Protocol

Image acquisition

Participants were scanned using a Philips Achieva 3.0 Tesla MRI system at the University of California, Irvine using an 8-channel SENSE receive only head coil and fitted padding to minimize head movements.

A single T1-weighted magnetization-prepared rapid gradient echo (MP-RAGE) scan was acquired using the following parameters: time repetition (TR)/time echo (TE) = 11/4.6 ms, field of view (FOV) = 240 × 231 mm, flip angle = 18°, 200 sagittal slices, and 0.75 mm^3 spatial resolution.

Three diffusion-weighted scans were acquired for each of four gradient values (b = 500, 1000, 2000 and 2500 s/mm^2). For each of the 12 scans, gradients were applied in 10 orthogonal directions, with one image having no diffusion weighting (b = 0). This yielded a total of 120 diffusion-weighted and 12 non-diffusion-weighted images. The following parameters were used for all 12 scans: TR/TE = 2174-2734/94 ms, FOV = 128 × 128 mm, 80 axial slices, 1.69 mm^3 spatial resolution, and the total scan time was approximately 50 minutes per subject.

Region of interest segmentation

The hippocampus was defined on each participant's MP-RAGE using FMRIB Software Library (FSL) Integrated Registration and Segmentation Tool (FIRST; Patenaude, Smith, Kennedy, & Jenkinson, 2011), which automatically segmented bilateral hippocampus using shape/appearance models with default boundary correction. The 3-stage affine registration was used to improve segmentation compared to the default

FIRST settings. In the first stage, the subject's MP-RAGE image is aligned to standard space (Montreal Neurological Institute; MNI) using an affine transformation. In the second stage, this transformation is linearly aligned to a subcortical mask in MNI space. In the third stage, a dilated hippocampal mask is aligned to refine the registration. Quality control of this segmentation, which included checks for coverage limited to the hippocampal gray matter region and allowing no more than a 1-2 voxel shift of the mask into the surrounding areas, were done by a trained researcher blinded to participant age and did not yield notable age differences.

Diffusion data processing

For each participant, all diffusion data were pre-processed using Analysis of Functional NeuroImages (AFNI) to remove non-brain tissue and generate a whole brain mask from the first non-diffusion weighted image (b0 image), and Advanced Normalization Tools (ANTs, Avants et al. 2009) to correct for gross motion by aligning all diffusion images to the b0 image. This preprocessed data from all diffusion scans (30 orthogonal directions for each of four gradient values) were used as input for both the single-tensor and NODDI analyses. Although these data were not corrected for bias field distortions, we replicated the age effects of interest in a separate sample with this correction (see Supplementary Material).

Single-tensor DTI analyses were completed using FSL dtifit. A single diffusion tensor was estimated at each voxel within a whole brain mask. The output included voxel-wise images for FA and MD.

Multi-compartment NODDI analyses were completed using the default settings in the NODDI toolbox (http://mig.cs.ucl.ac.uk/index.php?n=Tutorial.NODDImatlab). The diffusion signal for each voxel was separated into restricted, hindered, and free diffusion compartments using a two-stage approach (Tariq, Schneider, Alexander, Gandini Wheeler-Kingshott, & Zhang, 2016, Zhang et al., 2012). In the first stage, the total signal is separated into non-free and free diffusion sources of diffusion, with the latter being modeled as an isotropic sphere (also known as fISO). In the second stage, the remaining signal is then separated into restricted and hindered source of diffusion, modeled as a set of sticks (also known as NDI) and the dispersion of the sticks (also known as ODI), respectively. Restricted (or Gaussian) diffusion occurs when the movement of water molecules is constrained by the presence of impermeable barriers, whereas hindered (or non-Gaussian) diffusion occurs when their movement is constrained by the presence of partially permeable barriers (Martin, 2013; Morozov et al., 2020; Raja, Rosenberg, & Caprihan, 2019). Thus, modeling restricted diffusion as a set of sticks is intended to capture restricted diffusion within neurons and glia (i.e., intracellular diffusion). Modeling hindered diffusion as dispersion of those sticks is intended to capture hindered diffusion around those structures (i.e., extracellular diffusion). The output included voxel-wise images for restricted, hindered, and free diffusion. The scale of all NODDI measures range from 0-1.

To extract hippocampal gray matter integrity metrics for each participant, their MP-RAGE was linearly aligned to their b0 image using FSL's flirt command. This transformation was then applied to align the FIRST segmented bilateral hippocampus to

diffusion space. Quality control of this co-registration was completed as outlined above and did not yield notable age group differences. The aligned segmentations were binarized, creating a bilateral hippocampus mask. Unthresholded FA and MD metrics were obtained by multiplying the bilateral hippocampus mask by the corresponding voxel-wise DTI image and then taking the average across voxels. Free diffusion was obtained by multiplying the bilateral hippocampus mask by the corresponding voxel-wise NODDI image and then taking the average across voxels. Remaining diffusion metrics were limited to voxels with sufficient cellular fraction (>10%) by excluding voxels with free diffusion > 0.9 from the bilateral hippocampus mask. Measures of restricted and hindered diffusion were obtained by multiplying this thresholded bilateral hippocampus mask by the corresponding voxel-wise NODDI images and then taking the average across voxels. Finally, to assess the effect of free water on DTI measures, thresholded FA and MD were obtained by multiplying the thresholded hippocampus mask by the corresponding voxel-wise DTI image and then taking the average across voxels.

Statistical Analyses

All statistical analyses were run using Prism (Version 7.0d; GraphPad Software, La Jolla California USA), except for the logistic regression run using SPSS (Version 24.0; IBM, Armonk, NY, USA). For all analyses, the significance threshold was set to $p < 0.05$.

Age group differences in single-tensor DTI (FA, MD) and multi-compartment NODDI (restricted, hindered, free diffusion) metrics were assessed using separate independent sample *t*-tests. The effect of free diffusion on each DTI metric was assessed

using an Age Group (younger, older) × Thresholding (thresholded, unthresholded) ANOVA, with Age Group as a between-subject variable, and Thresholding as a within-subject variable. The ability of single-tensor and multi-compartment diffusion approaches to capture age-related variance were compared using a forward selection likelihood ratio (LR) logistic regression. The dependent variable was dichotomized age groups and independent variables were the unthresholded DTI and NODDI metrics. Variables were entered using the Forward Selection (LR) option in SPSS in which variables are entered in a stepwise manner based on the significance of the score statistic.

The moderating effect of age group on these relationships were assessed using separate linear regressions for each integrity metric (see Baron & Kenny, 1986). Relationships between hippocampal integrity and MST performance were assessed separately in each age group using linear regressions.

Results

Neuropsychological Test Performance

Age group differences in cognition were assessed using separate independent sample *t*-tests for each neuropsychological test (see Table 1). Results followed the expected pattern for healthy aging, with older adults performing worse than younger adults on measures of episodic memory (RAVLT, $t(47) = -3.26$, $p < 0.002$) and executive function (Trails B, $t(47) = 3.49$, $p < 0.001$; Stroop, $t(47) = -3.29$, $p < 0.002$), but not general cognition (MMSE). Although we screened for neurological conditions including

Mild Cognitive Impairment (MCI) and excluded participants with low general cognitions (MMSE < 28), we acknowledge that some older adults with preclinical dementia may be present in the sample.

Age Group Differences for Unthresholded Single-Tensor Metrics

Age group differences in hippocampal gray matter integrity were first assessed for traditional single-tensor DTI measures (unthresholded FA, unthresholded MD). Across separate independent sample *t*-tests, significant age group differences were observed, with older adults (0.17 ± 0.02) showing lower unthresholded FA than younger adults (0.18 ± 0.02), $t(47) = 3.64$, $p < 0.001$, $d = 0.5$. Effects were also significant for unthresholded MD (younger: 0.0007 ± 0.00002, older: 0.0007 ± 0.00003), $t(47) = 2.44$, $p < 0.02$, $d = 0.0$ (see Figure 1).

Age Group Differences for Thresholded Single-Tensor Metrics

Age group differences in hippocampal gray matter integrity were next assessed for single-tensor DTI measures that were thresholded to exclude voxels with excessively high NODDI free diffusion (thresholded FA, thresholded MD). Across separate independent sample *t*-tests, significant age group differences were observed, with older adults (0.17 ± 0.02) showing lower FA than younger adults (0.19 ± 0.02), $t(47) = 3.32$, $p < 0.002$, $d = 1.00$. The difference for thresholded MD was not significant, $t(47) = 1.40$, $p < 0.167$, $d = 0.0$ (see Figure 1).

Effect of Thresholding Single-Tensor Metrics

To assess whether accounting for free diffusion by thresholding the DTI metrics had an effect on the aforementioned age group differences in hippocampal gray matter

integrity, separate Age Group (younger, older) × Thresholding (thresholded, unthresholded) ANOVAs were conducted for each metric. As expected, results revealed significant main effects of Age Group for FA, $F(1, 47) = 12.11$, $p < 0.002$, but not MD, $p > 0.05$. Significant main effects of Thresholding were seen for both FA, $F(1, 47) = 31.92$, $p < 0.0001$, and MD, $F(1, 47) = 60.68$, $p < 0.0001$. Most importantly, significant age group × thresholding interactions for FA, $F(1, 47) = 7.18$, $p < 0.02$, and MD, $F(1, 47) = 14.96$, $p < 0.001$, revealed that age group differences were larger for unthresholded versus thresholded DTI metrics.

Age Group Differences for Multi-Compartment Metrics

Finally, age group differences in hippocampal gray matter integrity were assessed for multi-compartment NODDI measures (restricted, hindered, and free diffusion). Across separate independent sample *t*-tests, significant age group differences were observed, with older adults showing higher restricted (0.49 ± 0.03), $t(47) = 2.26$, $p < 0.03$, $d = 0.39$, hindered (0.46 ± 0.02), $t(47) = 4.14$, $p < 0.001$, $d = 1.00$, and free (0.34 ± 0.06), $t(47) = 3.24$, $p < 0.003$, $d = 1.27$ diffusion compared to younger adults (0.48 ± 0.02 restricted, 0.44 ± 0.02 hindered, 0.27 ± 0.05 free diffusion; see Figure 2).

Multi-Compartment Integrity Metrics Account for More Age-Related Variance than Single-Tensor Metrics

To determine whether multi-compartment integrity measures account for more age-related variance in hippocampal gray matter integrity than traditional single-tensor measures, DTI (unthresholded FA and MD) and NODDI (restricted, hindered, free diffusion) integrity measures were entered into a forward (LR) logistic regression.

Results revealed that the single best predictor of age group was hindered diffusion, *Nagelkerke* r^2 = 0.366, p <0.003. At the second step, adding free diffusion significantly increased the total explained variance, *Nagelkerke* r^2 = 0.643, p <0.002. Adding a third predictor did not lead to a significant increase in variance explained by the model. Thus, traditional DTI measures (FA, MD) were not included in the best model. These age effects were replicated in a separate dataset of younger and older adults (see Supplemental Materials).

Age Effects for Mnemonic Discrimination

Age group differences in MST performance were assessed using separate independent sample *t*-tests for the LDI and recognition measures. Consistent with previous work (Stark, Yassa, Lacy, & Stark, 2013b), results revealed that LDI was significantly reduced in older (0.28 ± 0.05) compared to younger (0.43 ± 0.04) adults, $t(39) = -2.58$, $p < 0.015$, $d = 3.31$, whereas recognition did not significantly differ between age groups (younger: 0.81 ± 0.07, older: 0.79 ± 0.11,), $t(39) = -0.51$, $p > 0.60$, $d = 0.22$ (see Figure 3).

Mnemonic Discrimination-Hippocampal Gray Matter Integrity Relationships

Regression analysis assessed whether age group was a moderator of the relationship between mnemonic discrimination and hippocampal integrity. Analyses were limited to the NODDI measures of hippocampal integrity that were most sensitive to age in the stepwise logistic regression analyses (hindered, free diffusion). Age group, diffusion, and the age group × diffusion interaction were used as predictor variables and LDI as the outcome variable (see Baron & Kenny, 1986). Results revealed that the

interaction term was significant for hindered diffusion ($\beta = 13.2$, $p < 0.002$) indicating that this relationship was significantly stronger for younger compared to older adults. Follow-up regression analyses in each age group revealed that LDI was significantly related to hippocampal hindered diffusion in younger adults, such that lower hindered diffusion was correlated with better mnemonic discrimination performance, $r^2 = 0.41$, $p < 0.006$ (see Figure 4). In older adults, the relationship between hindered diffusion and mnemonic discrimination performance did not reach significance, $r^2 = 0.12$, $p < 0.09$ (see Figure 4). Relationships between recognition and hippocampal integrity also did not approach significance, ps > 0.3.

For comparison, analyses were also run to assess whether age group was a moderator of the relationship between mnemonic discrimination and hippocampal integrity for unthresholded DTI measures (FA, MD). Age group, diffusion, and the age group × diffusion interaction were used as predictor variables and LDI as the outcome variable. Results revealed that the interaction term was significant for FA ($\beta = -4.1$, $p < 0.02$) indicating that this relationship was significantly stronger for younger compared to older adults. The interaction term for MD and free diffusion did not approach significance ($p > 0.41$). Follow-up regression analyses in each age group revealed that LDI was significantly related to hippocampal FA in younger adults, such that higher FA was correlated with better mnemonic discrimination performance, $r^2 = 0.28$, $p < 0.03$ (see Figure 5). In older adults, the relationship between FA and mnemonic discrimination performance did not reach significance, $r^2 = 0.03$, $p < 0.40$ (see Figure 5). Relationships between MD and LDI also did not approach significance ps > 0.28.

To compare whether NODDI (hindered diffusion) or DTI (FA) measures better captured mnemonic discrimination performance within younger adults, Steiger's Z test (Steiger, 1980) was used to compare the previously mentioned significant relationships. Results revealed that the relationship between hippocampal hindered diffusion and LDI was significantly stronger than the relationship between hippocampal FA and LDI, $Z = -2.92$, $p < 0.004$.

Discussion

The current study aimed to directly compare the sensitivity of single-tensor (DTI) and multi-compartment (NODDI) diffusion measures as they relate to age within hippocampal gray matter and to assess whether these measures predict episodic memory performance. Results revealed several major findings, each of which will be discussed in more detail below. First, we demonstrated that thresholding DTI metrics (FA, MD) to account for free diffusion significantly attenuates the effect of age on hippocampal gray matter integrity. Second, we showed that NODDI metrics (hindered and free diffusion) account for more age-related variance in hippocampal gray matter integrity than DTI metrics. These findings were replicated in a separate dataset (see Supplementary Material), highlighting the robustness of these age effects in light of different diffusion acquisition parameters and preprocessing steps. Third, we found a moderating effect of age group on the relationship between hippocampal gray matter integrity and mnemonic discrimination, such that lower hindered diffusion was related to better discrimination performance in younger but not older adults.

Traditional, single-tensor DTI was sensitive to age-related differences in hippocampal gray matter integrity. Older adults had significantly lower unthresholded FA and higher unthresholded MD than younger adults in bilateral hippocampus, consistent with an earlier report of similar effects for MD, albeit within an older sample (age 55-90; Den Heijer et al., 2012). Whereas age-related increases in MD are consistently reported for white matter (Head et al., 2004, Hugenschmidt et al., 2008, Salat et al., 2005), the findings are more mixed for gray matter. That is, some gray matter studies find age-related increase in MD (Carlesimo et al., 2010, Pereira et al., 2014, Den Heijer et al., 2012), others find no age difference (Cherubini et al., 2009), and yet other find mixed results depending on the region (Pfefferbaum et al. 2010, Salminen et al., 2016). Inferences that can be drawn about the neural substrates underlying differences in these scalar measures are limited (for example, see Wheeler-Kingshott & Cercignani, 2009). As in white matter, age-related decreases in hippocampal gray matter FA may result from degradation of the underlying tissue (e.g., loss of dendrites), reorganization of tissue (e.g., differences in dendritic layout), or some combination of the two; whereas age-related increases in hippocampal gray matter MD may indicate a loss of underlying tissue or an expansion of non-tissue space. Relative to the largely aligned microstructure in white matter (e.g. axons, neurofilaments), the organization of gray matter microstructure (e.g. dendrites, cell bodies, glia) is less coherent. We argue that, although both FA and MD were sensitive to age effects, the microstructural complexity of gray matter is not adequately captured by single-tensor diffusion models.

Our results further revealed that age-related differences in hippocampal gray matter integrity measured using single-tensor DTI were attenuated after accounting for free diffusion. Consistent with an earlier report using relative anisotropy (Càmara et al., 2007), older adults showed significantly lower hippocampal FA than younger adults after accounting for the CSF fraction. We observed no significant difference in thresholded MD, in bilateral hippocampus. Importantly, age group differences for our thresholded DTI measures were significantly smaller than for the unthresholded measures. By directly comparing age effects for the unthresholded and thresholded measures, our study revealed that single-tensor DTI measures are significantly influenced by the presence of free diffusion, which may originate from partial volume effects with cerebrospinal fluid in nearby ventricles (Chad et al., 2018b; Jeon et al., 2012; Metzler-Baddeley et al., 2012; Tohka, 2014) or cellular shrinkage or neurodegeneration (Ofori et al., 2015; Albi et al., 2016). Thus, rather than solely capturing the integrity of underlying gray matter tissue, MD in particular may be more sensitive to differences in free diffusion as evidenced by the lack of significant age-group differences after thresholding for free water.

Multi-compartment NODDI was also sensitive to age-related differences in hippocampal gray matter integrity, outperforming the ability of single-tensor DTI measures to capture these age effects. Older adults had significantly higher restricted, hindered and free diffusion in bilateral hippocampus relative to younger adults. Of note, these effects survived after controlling for volume (data not shown). A similar finding was previously reported for hindered diffusion using a lifespan sample (Nazeri et al., 2015). However, free diffusion was not assessed in that study, or controlled for in the

other diffusion compartments, as was done here. Although speculative, potential mechanisms for these age-related increases in hindered and free diffusion are neurodegeneration (e.g. age-related loss of apical dendrites, Dickstein, Weaver, Luebke, & Hof, 2013), loss of support cells like microglia (Robillard, Lee, Chiu, & MacLean, 2016), and increases in blood-brain barrier permeability (Elahy et al., 2015; Oakley & Tharakan, 2014). Younger adult brains are less likely to be affected by neurodegeneration but may be impacted by other cellular mechanisms (e.g. remodeling of synapses; Szebenyi et al., 2005, astrocyte activity; Hansson & Rönnbäck, 1995) which may also impact measures of hindered and free diffusion. The lack of an age-related decline in restricted diffusion however is consistent with evidence that normal aging is not accompanied by a loss of hippocampal neurons (Freeman et al., 2008). Importantly, when single-tensor DTI and multi-compartment NODDI measures were included in the same regression model, hindered diffusion was the strongest predictor of age followed by free diffusion, whereas no DTI measures survived in the model. This direct comparison supports the notion that NODDI and DTI are capturing different properties of hippocampal aging, and that these complex gray matter microstructures are best modeled using multiple NODDI diffusion compartments. Hippocampal NODDI metrics used here may serve as important biomarkers for normal brain aging and cognitive aging. In particular, future studies could build on this work to parse out if specific NODDI measures are sensitive to pathological aging such as MCI and Alzheimer's Disease.

The functional relevance of multi-compartment NODDI was further supported by finding that age moderated the relationship between hippocampal gray matter integrity

and mnemonic discrimination performance. Results revealed that decreased hindered diffusion within bilateral hippocampus was a significant predictor of better mnemonic discrimination in younger adults, but not older adults. This relationship was significantly stronger for hindered diffusion than FA, suggesting NODDI measures may be more informative for tracking cognition across a lifespan. However, these results were not replicated in a separate dataset that used a slightly different version of the MST, a younger sample that had a very restricted age range, and differences in imaging acquisition and analysis (see Supplementary Material), suggesting that additional research is needed to explore these age-brain-behavior relationships. Nonetheless, one interpretation of the age moderation is that, as a result of age-related degradation of the hippocampus, older adults may be relying less on this brain region, or on different brain regions, to perform the task relative to younger adult (Madden et al., 2004; Reuter-Lorenz, 2002). Support for this view will require longitudinal studies, which have not yet shown how brain-behavior relationships evolve over the lifespan. However, they do find that cognition and integrity later in life is predicted by early life cognition (Deary et al., 2006; Valdés Hernández et al., 2013; Wardlaw et al., 2011), indicating that the significant relationship between hippocampus integrity and mnemonic discrimination in young adults may inform the absence of this relationship in aging.

It is worth noting that some limitations to this study may contribute to the current findings. Most importantly, some model parameters for NODDI may be better suited for modeling diffusion in white matter compared to gray matter. For example, if the intrinsic diffusivity measure used to estimate diffusion within neurites and extracellular space is

assumed to be lower than the true value in gray matter, this could weaken age-group differences in hindered diffusion (for more discussion see Guerrero et al., 2019). However, other parameters of the NODDI model were specifically designed to model hindered and restricted diffusion in gray matter (e.g., mean orientation of Watson distribution (μ), and the axon diameter parameter, (α); Jespersen et al., 2007, Zhang et al., 2012). These measures may vary across brain regions and within individuals, which may affect estimates of diffusion reported here. Other limitations include having acquired these diffusion data in a single-phase encoding direction and only correcting for gross motion (not eddy current distortions). However, it is unlikely that these methodological approaches significantly impacted the current findings because we replicated all age effects in a separate dataset acquired in opposing phase encoding directions that allowed us to correct for bias distortions and preprocessed using more advanced eddy current corrections (see Supplementary Material).

In sum, the current study demonstrated that multi-compartment NODDI is more sensitive to age-related differences in hippocampal gray matter integrity than single-tensor DTI, likely due to its ability to more accurately model complex gray matter microstructure while accounting for free diffusion. Gray matter integrity as measured with NODDI hindered diffusion was also sensitive to mnemonic discrimination performance, particularly in younger adults. Taken together, our results suggest that caution should be taken when using DTI integrity measures to assess gray matter integrity as these measures are highly impacted by free diffusion. Instead, multi-compartment NODDI appears to be a more sensitive tool for assessing age-related

decline of hippocampal gray matter integrity and episodic memory performance across the lifespan. Although we focus on the hippocampus in this study, based on its involvement in mnemonic discrimination, future studies are needed to determine whether these findings also extend to other gray matter regions (e.g. cortex, basal ganglia).

Table 1
Demographic and neuropsychological data

	Younger	Older	Group Comparisons [t (p)]
Demographics			
N	24	25	
Mean Age	27.6 ± 5.1	70.4 ± 5.9	
Education	16.3 ± 2.3	17.4 ± 1.7	
Neuropsychological Tests			
MMSE	29.6 ± 0.7	29.5 ± 0.7	-0.34 (0.736)
RAVLT Total	62.0 ± 6.4	55.3 ± 7.9	**-3.26 (0.002)**
RAVLT Immediate	13.8 ± 1.4	12.3 ± 2.4	-2.76 (0.008)
RAVLT Delay	13.9 ± 1.2	12.1 ± 2.6	**-3.12 (0.003)**
GDS	2.0 ± 1.9	0.5 ± 1.0	**-3.45 (0.001)**
BDI	3.7 ± 3.9	2.4 ± 2.4	-1.34 (0.185)
Trails A	17.7 ± 5.1	25.0 ± 8.0	3.81 (0.001)
Trails B	48.8 ± 13.0	66.9 ± 22.1	**3.49 (0.001)**
Stroop Raw	112.8 ± 12.8	98.1 ± 18.1	**-3.29 (0.002)**
Digit Span Total	20.4 ± 4.4	18.4 ± 3.7	-1.73 (0.091)
PASE	180.9 ± 57.2	138.8 ± 48.4	-2.78 (0.008)

Note. Neuropsychological test scores (mean ± standard deviation) are presented separately for younger and older adults. Significant between-group differences (Bonferroni corrected for 11 comparisons, $p < 0.005$ are indicated in bolded text. MMSE = Mini-Mental State Examination, RAVLT = Ray Auditory Verbal Learning Task, GDS= Geriatric Depression Scale, BDI=Beck Depression Inventory, PASE= physical activity scale for the elderly.

Figure 1
Age group differences in single-tensor DTI measures of hippocampal gray matter integrity shown separately for unthresholded (top row) and thresholded (bottom row) measures of fractional anisotropy and mean diffusivity. Group differences were significant for FA, thresholded FA and MD. Thresholded MD did not show significant differences.

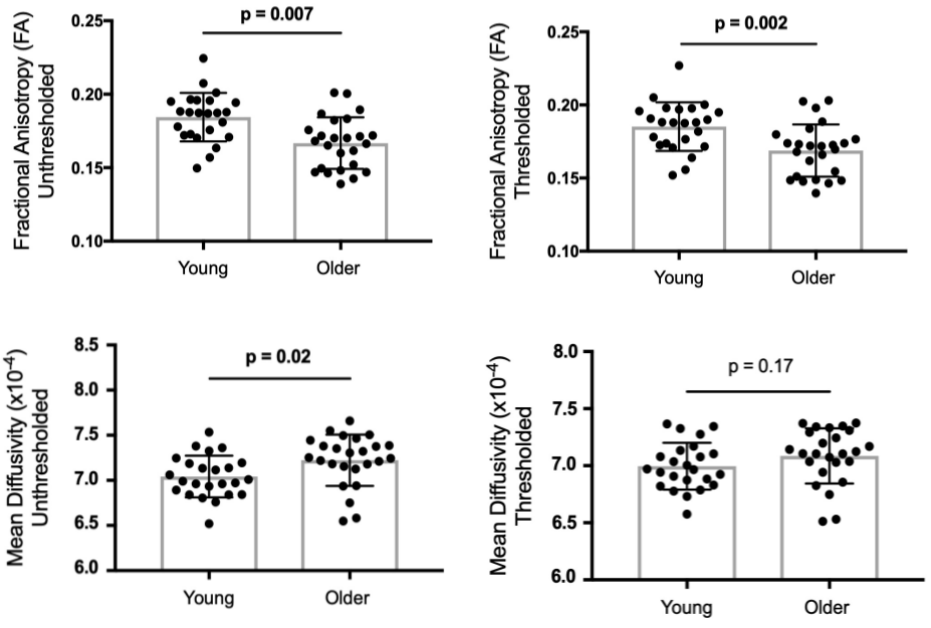

Figure 2
Age group differences in multi-compartment NODDI measures of hippocampal gray matter integrity shown separately for restricted (top), hindered (middle) and free diffusion (bottom). Group differences were significant for restricted, hindered and free diffusion

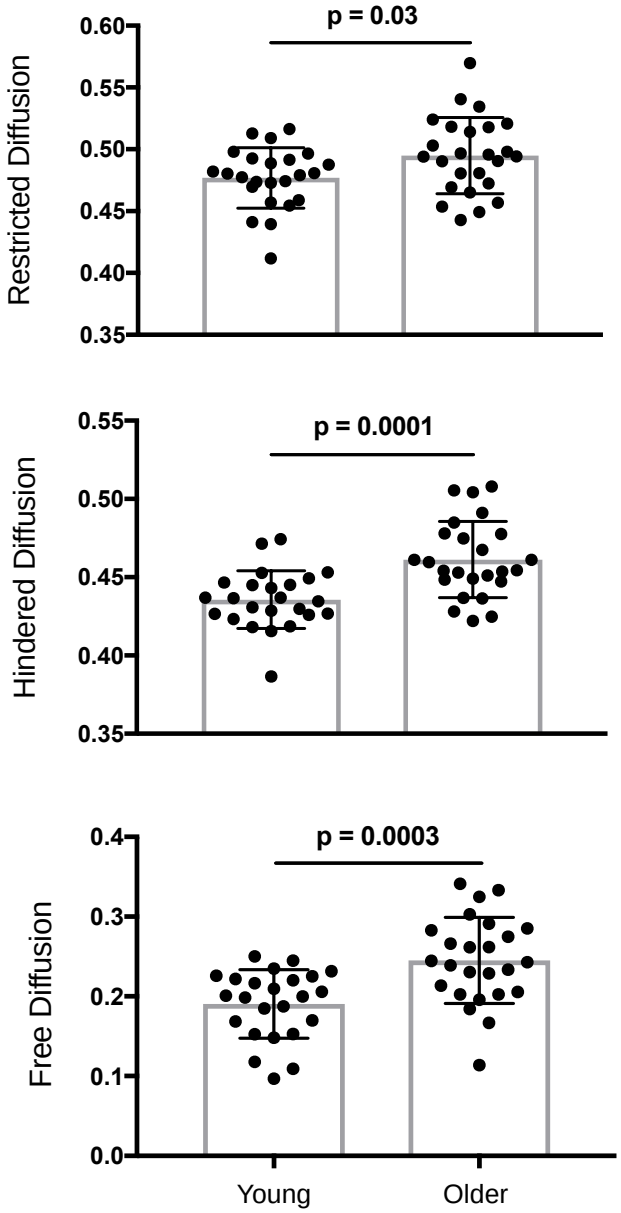

Table 2

Performance of single-tensor and multi-compartment integrity measures to account for age-related variance were compared using forward likelihood ratio logistic regression. Hindered and free diffusion measures captured the most age-related variance. All other predictors were excluded from the model.

Model	Variable	B	S.E.	Wald	Sig.	Negelkerke R Square
1	Hindered	61.799	20.07	9.481	0.002	0.366
2	Free Diffusion	37.101	12.511	8.794	0.003	0.643
	Hindered	78.046	24.063	10.519	0.001	

Predicted Variable: Age, dichotomized. B = Intercept, S.E.= Standard Error, Wald = Wald chi-square test, Sig.= Significance

Figure 3
Age group differences in Mnemonic Similarity Task performance shown separately for mnemonic discrimination (left) and recognition memory (right). Group differences were significant for mnemonic discrimination performance but not recognition.

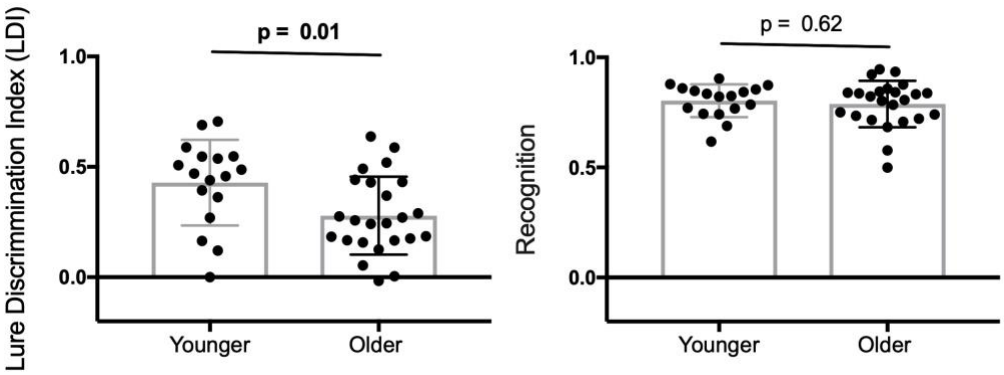

Figure 4
Relationships between mnemonic discrimination performance and NODDI hindered diffusion in hippocampus are shown separately for younger (left) and older (right) adults. For younger adults, hindered diffusion was significantly related to mnemonic discrimination (two-tailed).

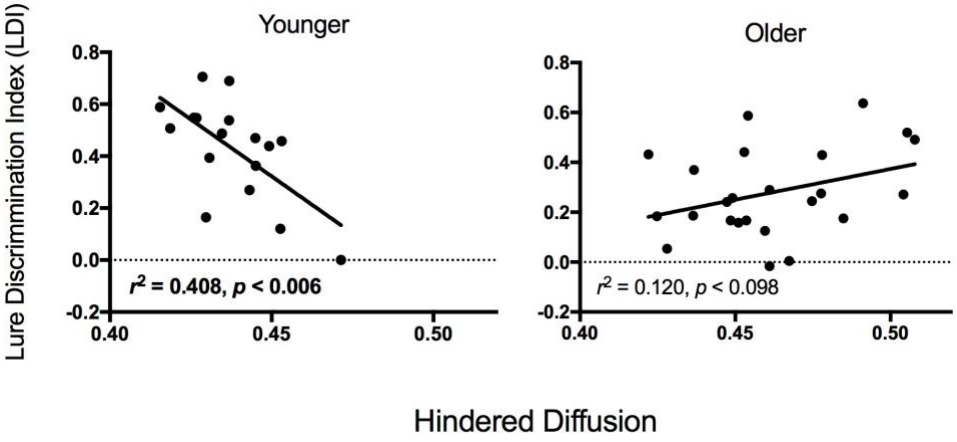

Figure 5
Relationships between mnemonic discrimination performance and DTI measures in hippocampus are shown separately for younger (left) and older (right) adults. For younger adults, FA, the relationship integrity and mnemonic discrimination approached significance (two-tailed).

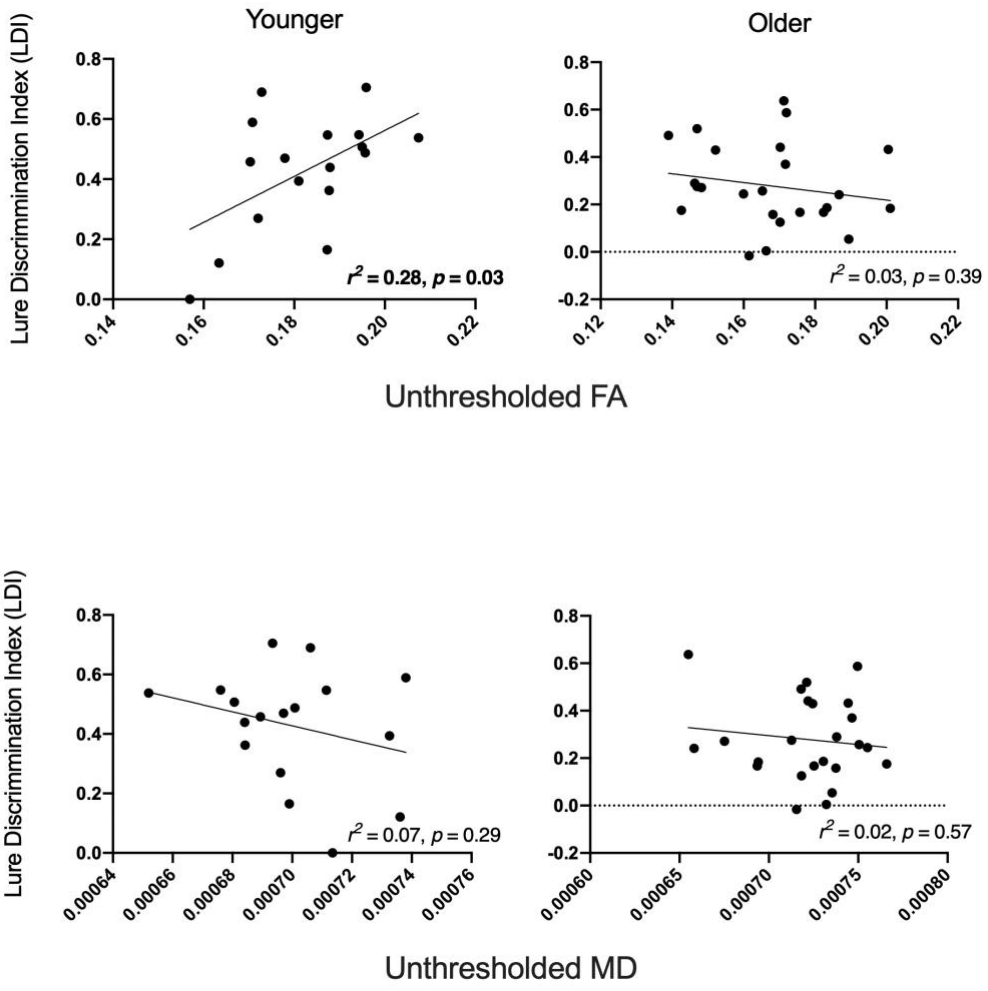

References

Albi, A., Pasternak, O., Minati, L., Marizzoni, M., Bartrés-Faz, D., Bargalló, N., … Jovicich, J. (2016). Free water elimination improves test-retest reproducibility of diffusion tensor imaging indices in the brain: A longitudinal multisite study of healthy elderly subjects. *Human Brain Mapping*, *38*(1), 12–26. https://doi.org/10.1002/hbm.23350

Barnes, J., Scahill, R. I., Boyes, R. G., Frost, C., Lewis, E. B., Rossor, C. L., … Fox, N. C. (2004). Differentiating AD from aging using semiautomated measurement of hippocampal atrophy rates. *NeuroImage*, *23*(2), 574–581. https://doi.org/10.1016/j.neuroimage.2004.06.028

Baron, R. M., & Kenny, D. A. (1986). The Moderator-Mediator Variable Distinction in Social Psychological Research: Conceptual, Strategic, and Statistical Considerations. *Journal of Pe~nality and Social Psychology*, *51*(6), 1173–1182. Retrieved from http://www.sesp.org/files/The Moderator-Baron.pdf

Beaulieu, C. (2002). The basis of anisotropic water diffusion in the nervous system - a technical review. *NMR in Biomedicine*, *15*(7–8), 435–455. https://doi.org/10.1002/nbm.782

Bennett, I. J., Huffman, D. J., & Stark, C. E. L. (2015). Limbic tract integrity contributes to pattern separation performance across the lifespan. *Cerebral Cortex*, *25*(9), 2988–2999. https://doi.org/10.1093/cercor/bhu093

Bennett, I. J., & Stark, C. E. L. (2016). Mnemonic discrimination relates to perforant path integrity: An ultra-high resolution diffusion tensor imaging study. *Neurobiology of Learning and Memory*, *129*, 107–112. https://doi.org/10.1016/j.nlm.2015.06.014

Càmara, E., Bodammer, N., Rodríguez-Fornells, A., & Tempelmann, C. (2007). Age-related water diffusion changes in human brain: A voxel-based approach. *NeuroImage*, *34*(4), 1588–1599. https://doi.org/10.1016/j.neuroimage.2006.09.045

Carlesimo, G. A., Cherubini, A., Caltagirone, C., & Spalletta, G. (2010). Hippocampal mean diffusivity and memory in healthy elderly individuals: A cross-sectional study. *Neurology*, *74*(3), 194–200. https://doi.org/10.1212/WNL.0b013e3181cb3e39

Chad, J. A., Pasternak, O., Salat, D. H., & Chen, J. J. (2018). Re-examining age-related differences in white matter microstructure with free-water corrected diffusion tensor imaging. *Neurobiology of Aging*, *71*, 161–170. https://doi.org/10.1016/j.neurobiolaging.2018.07.018

Cherubini, A., Péran, P., Caltagirone, C., Sabatini, U., & Spalletta, G. (2009). Aging of subcortical nuclei: Microstructural, mineralization and atrophy modifications measured in vivo using MRI. *NeuroImage*, *48*(1), 29–36. https://doi.org/10.1016/j.neuroimage.2009.06.035

Clarke, L. E., Liddelow, S. A., Chakraborty, C., Münch, A. E., Heiman, M., & Barres, B. A. (2018). Normal aging induces A1-like astrocyte reactivity. *Proceedings of the National Academy of Sciences*, *115*(8), E1896–E1905. https://doi.org/10.1073/pnas.1800165115

de Lange, A. M. G., Bråthen, A. C. S., Grydeland, H., Sexton, C., Johansen-Berg, H., Andersson, J. L. R., … Walhovd, K. B. (2016). White-matter integrity as a marker for cognitive plasticity in aging. *Neurobiology of Aging*, *47*, 74–82. https://doi.org/10.1016/j.neurobiolaging.2016.07.007

Den Heijer, T., der Lijn, F. van, Vernooij, M. W., de Groot, M., Koudstaal, P. J., der Lugt, A. van, … Breteler, M. M. B. (2012). Structural and diffusion MRI measures of the hippocampus and memory performance. *NeuroImage*, *63*(4), 1782–1789. https://doi.org/10.1016/j.neuroimage.2012.08.067

Dickstein, D. L., Weaver, C. M., Luebke, J. I., & Hof, P. R. (2013). Dendritic spine changes associated with normal aging. *Neuroscience*, *251*, 21–32. https://doi.org/10.1016/j.neuroscience.2012.09.077

Doxey, C. R., & Kirwan, C. B. (2015). Structural and functional correlates of behavioral pattern separation in the hippocampus and medial temporal lobe. *Hippocampus*, *25*(4), 524–533. https://doi.org/10.1002/hipo.22389

Elahy, M., Jackaman, C., Mamo, J. C., Lam, V., Dhaliwal, S. S., Giles, C., … Takechi, R. (2015). Blood-brain barrier dysfunction developed during normal aging is associated with inflammation and loss of tight junctions but not with leukocyte recruitment. *Immunity & Ageing : I & A*, *12*, 2. https://doi.org/10.1186/s12979-015-0029-9

Freeman, S. H., Kandel, R., Cruz, L., Rozkalne, A., Newell, K., Frosch, M. P., … Hyman, B. T. (2008). Preservation of neuronal number despite age-related cortical brain atrophy in elderly subjects without alzheimer disease. *Journal of Neuropathology and Experimental Neurology*, *67*(12), 1205–1212. https://doi.org/10.1097/NEN.0b013e31818fc72f

Fukutomi, H., Glasser, M. F., Zhang, H., Autio, J. A., Coalson, T. S., Okada, T., … Hayashi, T. (2018). Neurite imaging reveals microstructural variations in human cerebral cortical gray matter. *NeuroImage*, *182*, 488–499. https://doi.org/10.1016/J.NEUROIMAGE.2018.02.017

Guerrero, J. M., Adluru, N., Bendlin, B. B., Goldsmith, H. H., Schaefer, S. M., Davidson, R. J., … Alexander, A. L. (2019). Optimizing the intrinsic parallel diffusivity in NODDI: An extensive empirical evaluation. *PLOS ONE*, *14*(9), e0217118. https://doi.org/10.1371/journal.pone.0217118

Gunning-Dixon, F. M., Brickman, A. M., Cheng, J. C., & Alexopoulos, G. S. (2009). Aging of cerebral white matter: A review of MRI findings. *International Journal of Geriatric Psychiatry*, *24*(2), 109–117. https://doi.org/10.1002/gps.2087

Hansson, E., & Rönnbäck, L. (1995). Astrocytes in glutamate neurotransmission. *FASEB Journal : Official Publication of the Federation of American Societies for Experimental Biology*, *9*(5), 343–350. https://doi.org/10.1096/fasebj.9.5.7534736

Hassan, M. K., ul-Haq, M., Amin, M., Tahirullah, Nawaz, A., & Ullah, H. (2014). Association between baseline parameters and end of treatment response to combination of conventional interferon & ribavirin in patients with chronic hepatitis C. *Journal of Postgraduate Medical Institute*, *28*(2), 149–153. https://doi.org/10.1016/j.neuron.2006.08.012

Jeon, T., Mishra, V., Uh, J., Weiner, M., Hatanpaa, K. J., White, C. L., … Huang, H. (2012). Regional changes of cortical mean diffusivities with aging after correction of partial volume effects. *NeuroImage*, *62*(3), 1705–1716. https://doi.org/10.1016/j.neuroimage.2012.05.082

Jespersen, S. N., Kroenke, C. D., Østergaard, L., Ackerman, J. J. H., & Yablonskiy, D. A. (2007). Modeling dendrite density from magnetic resonance diffusion measurements. *NeuroImage*, *34*(4), 1473–1486. https://doi.org/10.1016/j.neuroimage.2006.10.037

Kaden, E., Kelm, N. D., Carson, R. P., Does, M. D., & Alexander, D. C. (2016). Multi-compartment microscopic diffusion imaging. *NeuroImage*, *139*, 346–359. https://doi.org/10.1016/j.neuroimage.2016.06.002

Kohama, S. G., Goss, J. R., Finch, C. E., & McNeill, T. H. (1995). Increases of glial fibrillary acidic protein in the aging female mouse brain. *Neurobiology of Aging*, *16*(1), 59–67. https://doi.org/10.1016/0197-4580(95)80008-F

Lister, J. P., & Barnes, C. A. (2009). Neurobiological changes in the hippocampus during normative aging. *Archives of Neurology*, *66*(7), 829–833. https://doi.org/10.1001/archneurol.2009.125

Madden, D. J., Bennett, I. J., Burzynska, A., Potter, G. G., Chen, N., & Song, A. W. (2012). Diffusion tensor imaging of cerebral white matter integrity in cognitive

aging. *Biochimica et Biophysica Acta (BBA) - Molecular Basis of Disease*, *1822*(3), 386–400. https://doi.org/10.1016/j.bbadis.2011.08.003

Madden, D. J., Whiting, W. L., Huettel, S. A., White, L. E., MacFall, J. R., & Provenzale, J. M. (2004). Diffusion tensor imaging of adult age differences in cerebral white matter: relation to response time. *NeuroImage*, *21*(3), 1174–1181. https://doi.org/10.1016/J.NEUROIMAGE.2003.11.004

Martin, M. (2013). Measuring restriction sizes using diffusion weighted magnetic resonance imaging: a review. *Magnetic Resonance Insights*, *6*, 59–64. https://doi.org/10.4137/MRI.S11149

Metzler-Baddeley, C., O'Sullivan, M. J., Bells, S., Pasternak, O., & Jones, D. K. (2012). How and how not to correct for CSF-contamination in diffusion MRI. *NeuroImage*, *59*(2), 1394–1403. https://doi.org/10.1016/J.NEUROIMAGE.2011.08.043

Morozov, S., Sergunova, K., Petraikin, A., Akhmad, E., Kivasev, S., Semenov, D., … Morozov, A. (2020). Diffusion processes modeling in magnetic resonance imaging. *Insights into Imaging*, *11*(1), 60. https://doi.org/10.1186/s13244-020-00863-w

Nazeri, A., Mulsant, B. H., Rajji, T. K., Levesque, M. L., Pipitone, J., Stefanik, L., … Voineskos, A. N. (2017). Gray Matter Neuritic Microstructure Deficits in Schizophrenia and Bipolar Disorder. *Biological Psychiatry*, *82*(10), 726–736. https://doi.org/10.1016/j.biopsych.2016.12.005

Oakley, R., & Tharakan, B. (2014). Vascular Hyperpermeability and Aging. *Aging and Disease*, *5*(2), 114–125. https://doi.org/10.14336/AD.2014.0500114

Ofori, E., Pasternak, O., Planetta, P., Burciu, R., Snyder, A., Febo, M., … Vaillancourt, D. (2015). Increased free-water in the substantia nigra of Parkinson's disease: a single-site and multi-site study. *Neurobiol Aging*, *36*(2), 1097–1104. https://doi.org/10.1016/j.neurobiolaging.2014.10.029

Park, D. C., & Reuter-Lorenz, P. (n.d.). The Adaptive Brain: Aging and Neurocognitive Scaffolding. https://doi.org/10.1146/annurev.psych.59.103006.093656

Patenaude, B., Smith, S. M., Kennedy, D. N., & Jenkinson, M. (2011). A Bayesian model of shape and appearance for subcortical brain segmentation. https://doi.org/10.1016/j.neuroimage.2011.02.046

Pereira, J. B., Valls-Pedret, C., Ros, E., Palacios, E., Falcón, C., Bargalló, N., … Junque, C. (2014). Regional vulnerability of hippocampal subfields to aging measured by structural and diffusion MRI. *Hippocampus*, *24*(4), 403–414. https://doi.org/10.1002/hipo.22234

Pfefferbaum, A., Adalsteinsson, E., Rohlfing, T., & Sullivan, E. V. (2010). Diffusion tensor imaging of deep gray matter brain structures: Effects of age and iron concentration. *Neurobiology of Aging*, *31*(3), 482–493. https://doi.org/10.1016/j.neurobiolaging.2008.04.013

Rae, C. L., Davies, G., Garfinkel, S. N., Gabel, M. C., Dowell, N. G., Cercignani, M., … Critchley, H. D. (2017). Archival Report Deficits in Neurite Density Underlie White Matter Structure Abnormalities in First-Episode Psychosis. *Biological Psychiatry*, *82*, 716–725. https://doi.org/10.1016/j.biopsych.2017.02.008

Raja, R., Rosenberg, G., & Caprihan, A. (2019). Review of diffusion MRI studies in chronic white matter diseases. *Neuroscience Letters*, *694*, 198–207. https://doi.org/10.1016/j.neulet.2018.12.007

Rathi, Y., Pasternak, O., Savadjiev, P., Michailovich, O., Bouix, S., Kubicki, M., … Shenton, M. E. (2014). Gray matter alterations in early aging: A diffusion magnetic resonance imaging study. *Human Brain Mapping*, *35*(8), 3841–3856. https://doi.org/10.1002/hbm.22441

Raz, N., Lindenberger, U., Rodrigue, K. M., Kennedy, K. M., Head, D., Williamson, A., … Acker, J. D. (2005). Regional brain changes in aging healthy adults: General trends, individual differences and modifiers. *Cerebral Cortex*, *15*(11), 1676–1689. https://doi.org/10.1093/cercor/bhi044

Reuter-Lorenz, P. A. (2002). New visions of the aging mind and brain. *Trends in Cognitive Sciences*, *6*(9), 394–400. https://doi.org/10.1016/S1364-6613(02)01957-5

Robillard, K. N., Lee, K. M., Chiu, K. B., & MacLean, A. G. (2016). Glial cell morphological and density changes through the lifespan of rhesus macaques. *Brain, Behavior, and Immunity*, *55*, 60–69. https://doi.org/10.1016/j.bbi.2016.01.006

Salminen, L. E., Conturo, T. E., Laidlaw, D. H., Cabeen, R. P., Akbudak, E., Lane, E. M., … Paul, R. H. (2016). Regional age differences in gray matter diffusivity among healthy older adults. *Brain Imaging and Behavior*, *10*(1), 203–211. https://doi.org/10.1007/s11682-015-9383-7

Sasson, E., Doniger, G. M., Pasternak, O., Tarrasch, R., & Assaf, Y. (2012). Structural correlates of cognitive domains in normal aging with diffusion tensor imaging. *Brain Structure and Function*, *217*(2), 503–515. https://doi.org/10.1007/s00429-011-0344-7

Scahill, R. I., Frost, C., Jenkins, R., Whitwell, J. L., Rossor, M. N., & Fox, N. C. (2003). A Longitudinal Study of Brain Volume Changes in Normal Aging Using Serial

Registered Magnetic Resonance Imaging. *Archives of Neurology*, *60*(7), 989. https://doi.org/10.1001/archneur.60.7.989

Stark, S. M., Yassa, M. A., Lacy, J. W., & Stark, C. E. L. (2013a). A task to assess behavioral pattern separation (BPS) in humans: Data from healthy aging and mild cognitive impairment. *Neuropsychologia*, *51*(12), 2442–2449. https://doi.org/10.1016/j.neuropsychologia.2012.12.014

Stark, S. M., Yassa, M. A., Lacy, J. W., & Stark, C. E. L. (2013b). A task to assess behavioral pattern separation (BPS) in humans: Data from healthy aging and mild cognitive impairment. *Neuropsychologia*, *51*(12), 2442–2449. https://doi.org/10.1016/J.NEUROPSYCHOLOGIA.2012.12.014

Steiger, J. H. (1980). Tests for comparing elements of a correlation matrix. *Psychological Bulletin*, *87*(2), 245–251. https://doi.org/10.1037/0033-2909.87.2.245

Szebenyi, G., Bollati, F., Bisbal, M., Sheridan, S., Faas, L., Wray, R., … Brady, S. T. (2005). Activity-Driven Dendritic Remodeling Requires Microtubule-Associated Protein 1A. *Current Biology*, *15*(20), 1820–1826. https://doi.org/10.1016/j.cub.2005.08.069

Tariq, M., Schneider, T., Alexander, D. C., Gandini Wheeler-Kingshott, C. A., & Zhang, H. (2016). Bingham-NODDI: Mapping anisotropic orientation dispersion of neurites using diffusion MRI. https://doi.org/10.1016/j.neuroimage.2016.01.046

Tohka, J. (2014). Partial volume effect modeling for segmentation and tissue classification of brain magnetic resonance images: A review. *World Journal of Radiology*, *6*(11), 855–864. Retrieved from http://www.ncbi.nlm.nih.gov/pubmed/25431640

Weston, P. S. J., Simpson, I. J. A., Ryan, N. S., Ourselin, S., & Fox, N. C. (2015). Diffusion imaging changes in grey matter in Alzheimer's disease: a potential marker of early neurodegeneration. *Alzheimer's Research & Therapy*, *7*(1), 47. https://doi.org/10.1186/s13195-015-0132-3

Wheeler-Kingshott, C. A. M., & Cercignani, M. (2009). About "axial" and "radial" diffusivities. *Magnetic Resonance in Medicine*, *61*(5), 1255–1260. https://doi.org/10.1002/mrm.21965

Yassa, M. A., Muftuler, L. T., & Stark, C. E. L. (2010). Ultrahigh-resolution microstructural diffusion tensor imaging reveals perforant path degradation in aged humans in vivo. *Proceedings of the National Academy of Sciences of the United States of America*, *107*(28), 12687–12691. https://doi.org/10.1073/pnas.1002113107

Yusuf A. Bhagat and Christian Beaulieu, P. (2004). Diffusion Anisotropy in Subcortical White Matter and Cortical Gray Matter: Changes With Aging and the Role of CSF-Suppression. *JOURNAL OF MAGNETIC RESONANCE IMAGING*. Retrieved from https://onlinelibrary.wiley.com/doi/pdf/10.1002/jmri.20102

Zhang, H., Schneider, T., Wheeler-Kingshott, C. A., & Alexander, D. C. (2012). NODDI: Practical in vivo neurite orientation dispersion and density imaging of the human brain. *NeuroImage*, *61*(4), 1000–1016. https://doi.org/10.1016/j.neuroimage.2012.03.072

Chapter 2: NODDI Diffusion Compartments in Gray Matter Are Sensitive to Age and Selective to Mnemonic Discrimination and Recall Memory

Abstract

To better understand how brain wide gray matter microstructure differs across the lifespan and relates to memory performance, the current study uses multi-compartment diffusion imaging in cortical and subcortical regions and examines relationships to recall and recognition performance in 78 young (20.50 ± 1.95 years old) and 68 older adults (73.22 ± 5.96 years old). Following replication of age-related differences in cortical and subcortical diffusion measures, frontal lobe free water was found to be the single best predictor of age. This is consistent with existing cognitive aging hypotheses such as the frontal lobe hypothesis. Regarding memory performance, multi-compartment diffusion measures in frontal lobe, hippocampus, putamen, and occipital lobe significantly explained differences in in recall, recognition, and mnemonic discrimination performance. The pattern of results in hippocampus demonstrated that tissue compartments (restricted and hindered diffusion) were selective to different facets of memory, restricted diffusion best predicted delayed recall whereas hindered diffusion best predicted mnemonic discrimination. In contrast, relationships to performance in frontal and occipital lobes, and putamen demonstrated that the non-tissue (free water) compartment was most sensitive to delayed recall and recognition performance. This suggests that multi-compartment diffusion measures may be sensitive to different features of gray matter microstructure (e.g., astrogliosis, dendritic complexity and cerebral spinal fluid), which vary by brain region and are functionally selective to memory measures.

Introduction

One of primary challenges in cognitive aging is that the effect of age on gray matter microstructure and the resulting contributions to memory decline are not fully understood; this may ultimately make it difficult to understand normal and pathological (e.g., dementia) memory declines across the lifespan. To help close this knowledge gap, the current study uses diffusion imaging to characterize differences in gray matter microstructure and examine relationships between microstructure and memory performance, using healthy young and older adults. Traditional diffusion tensor imaging (DTI) is disadvantaged in gray matter, given its highly heterogeneous organization compared to white matter tracts. Our group previously demonstrated that a multi-compartment approach (Neurite Orientation Dispersion and Density Imaging, NODDI; Zhang, Schneider, Wheeler-Kingshott, & Alexander, 2012) outperformed diffusion tensor imaging (DTI) in capturing age and memory performance (Venkatesh, Stark, Stark, & Bennett, 2020) in the hippocampus. In the current study, we explore if this pattern extends to cortex and basal ganglia, while also testing existing hypotheses of cognitive aging, like the frontal lobe hypothesis which suggests that anterior regions of the brain are most susceptible to age-related deterioration (frontal lobe hypothesis; Dempster, 1992; West, 1996). NODDI can be sensitive to this effect by measuring the separate contributions of tissue and non-tissue (i.e., free water) compartments to age-related differences in cortical and subcortical brain regions. To assess a functional consequence of microstructure differences, relationships to memory performance will be examined for recall, recognition, and mnemonic discrimination performance. Using this approach, this

will be the first study to comprehensively characterize brain wide gray matter microstructure and relationships to memory performance using single-tensor and multi-compartment diffusion imaging, in young and older adults.

Previous studies using DTI have demonstrated that these diffusion measures are sensitive to age, however the biological contributors of these age group differences in gray matter have been difficult to understand. The aging studies which have used DTI in gray matter (Bhagat & Beaulieu, 2004; Càmara, Bodammer, Rodríguez-Fornells, & Tempelmann, 2007; Carlesimo, Cherubini, Caltagirone, & Spalletta, 2010; Cherubini, Péran, Caltagirone, Sabatini, & Spalletta, 2009; Den Heijer et al., 2012; Pereira et al., 2014; Pfefferbaum, Adalsteinsson, Rohlfing, & Sullivan, 2010; Rathi et al., 2014) have found that fractional anisotropy (FA) and mean diffusivity (MD) show all possible relationships to age (increases, decreases, both or no changes). While the inconsistencies between studies may be due to differences in methodologies or populations, the more important concern is that DTI measures do not provide adequate information about the underlying neurobiology. Since FA and MD estimates are based on a tensor, numerous biological variables such as iron accumulation, different cell types (glia, neurons), and cerebral spinal fluid (CSF) can all affect a single measure of anisotropy (FA) or rate of diffusion (MD) in gray matter (Mori & Zhang, 2006; Pfefferbaum et al., 2010). Thus, it would be valuable to build on existing DTI results with a multi-compartment approach to gain better sensitivity to the underlying biological variables in gray matter.

Unlike tensor based modeling of diffusion, multi-compartment models like NODDI (H. Zhang et al., 2012) can distinguish between the tissue and non-tissue (free

water) compartments, which may provide greater sensitivity to age group differences in microstructure. NODDI models diffusion within a voxel into three primary compartments including restricted (also known as Intracellular Volume Fraction; ICVF), hindered (also known as Orientation Dispersion Index; ODI) and free (also known as Fraction of Isotropic diffusion; fISO) diffusion. These three compartments are defined by displacement and diffusivity patterns that would most closely reflect diffusion within intra- and extra-cellular spaces, and CSF, respectively. NODDI measures have been separately mapped on to a number of neurobiological features using histology, for example restricted diffusion has been associated with tau burden and cell density (Colgan et al., 2016; Grussu et al., 2017; Mao et al., 2020), hindered diffusion with microglial density and neurite complexity (Grussu et al., 2017; Yi et al., 2019), and free diffusion with free water volume (Gatto et al., 2018). Using NODDI, studies from our group among others have reported higher restricted and free diffusion in older adults compared to young in hippocampus and dorsal striatum (Franco, Petok, Langley, Hu, & Bennett, 2020; Kojima et al., 2014; Radhakrishnan, Stark, & Stark, 2020; Venkatesh, Stark, Stark, & Bennett, 2020), higher hindered diffusion in hippocampus (Nazeri et al., 2015; Venkatesh et al., 2020) and an age-related decrease in hindered diffusion within cortical lobes (Nazeri et al., 2015). Importantly, the free water compartment was found to outperform other diffusion measures in capturing age in white matter (Chad et al., 2018b) and hippocampal gray matter (Venkatesh et al., 2020). This is consistent with a growing body of literature (Chad et al., 2018; Ofori et al., 2015; Pasternak, Sochen, Gur, Intrator, & Assaf, 2009; Simon & Iliff, 2016, Gullett et al., 2020; Maillard et al., 2019) in white

matter, which suggests that free water accumulation is a hallmark of cognitive aging. The extension of this free water accumulation model to other gray matter regions including in cortex and basal ganglia would be informative for better understanding the effect of age across the brain.

Rather than being uniform across the brain, the frontal lobe hypothesis (Dempster, 1992; West, 1996) suggests that the effect of age-related deterioration is stronger in anterior portions of the brain compared to posterior portions. While this hypothesis originally referred to the selective deterioration of cognitive functions attributed to prefrontal regions, subsequent studies also support the idea of an anterior to posterior gradient of structural deterioration in volume (Raz et al., 2005; Resnick, Pham, Kraut, Zonderman, & Davatzikos, 2003) and white matter microstructure (Bennett, Madden, Vaidya, Howard, & Howard, 2010; Pfefferbaum, Adalsteinsson, & Sullivan, 2005). Using NODDI in cortical and subcortical gray matter, the frontal lobe hypothesis can also be assessed in gray matter microstructure.

Lastly, the current study will examine the functional consequences of age group differences in microstructure by investigation relationships to memory performance in both cortical and subcortical brain regions. The Rey Auditory Verbal Learning Task (RAVLT; Rey, 1941) and Mnemonic Similarity Task (MST; see Stark et al 2013) will be used to measure memory performance at varying levels of difficulty including recall, recognition, and mnemonic discrimination. Previous studies have shown age group differences in verbal recall performance to be larger than differences in recognition performance (Danckert & Craik, 2013; Rhodes, Greene, & Naveh-Benjamin, 2019),

perhaps because recall requires “self-initiated processing” (Craik, 1986), which may be selectively impaired by age-related deterioration. Some types of recognition may be more impaired than others for similar reasons, mnemonic discrimination is a form of recognition that is impaired in older adults compared to young (Stark & Stark, 2017; Stark et al., 2013a) and requires accurate discrimination between a current and previously seen image (Klippenstein, Stark, Stark, & Bennett, 2020). Studies examining the relationships between gray matter microstructure and memory performance have found that hippocampal MD and restricted diffusion were both negatively associated with delayed RAVLT recall (Carlesimo et al., 2010; Den Heijer et al., 2012; Radhakrishnan et al., 2020), whereas the relationship between MST performance and hippocampal hindered diffusion (Venkatesh et al., 2020) was moderated by age group. Evidence from functional magnetic resonance imaging (fMRI) have suggested that cortical regions, in addition to the hippocampus are also involved in memory performance (RAVLT; Goveas et al., 2011; Sala-Llonch et al., 2014, MST; Nash et al., 2021; Wais, Jahanikia, Steiner, Stark, & Gazzaley, 2017). The current study will examine this possibility using diffusion imaging in cortical and subcortical gray matter, including in sensory cortices for each task (auditory regions for RAVLT vs. visual for MST).

In summary, the current study will use brain wide diffusion imaging to characterize age-group differences in gray matter microstructure and relationships to memory performance. By examining single-tensor and multi-compartment diffusion approaches together, we will assess the relative sensitivity of NODDI to age-related differences in tissue (restricted, hindered diffusion) and free water compartments.

Further, we will investigate if gray matter diffusion measures can inform existing models of cognitive aging including the free water accumulation model (Chad et al., 2018b) and the frontal lobe hypothesis (West, 1996). To our knowledge, this is the first study to examine the relationships between gray matter diffusion measures and mnemonic discrimination (in addition to recall and recognition) in both cortical and subcortical regions. This approach will replicate previous findings in hippocampus while extending knowledge about how specific tissue compartments in hippocampus and other regions explain differences in memory performance. Overall, the current study will establish a comprehensive foundation for understanding individual and age-related differences in gray matter microstructure, and its functional consequences to memory performance.

Methods

Participants

Young and older adults were recruited from the University of California, Riverside (UCR) and surrounding communities and the UCR Institutional Review Board approved the experimental procedures. Prior to enrollment in the study, participants were screened over the phone for neurological conditions (e.g., depression, stroke), and scanner related contraindications (e.g., claustrophobia, pregnancy). All individuals provided informed consent prior to participation in this study and were compensated for their time.

General cognition was measured using the Montreal Cognitive Assessment (MoCA; Nasreddine et al., 2005) and Mini-Mental State Exam (MMSE; Folstein, Folstein, & McHugh, 1975) in a subset of young adults (n = 43). Participants included in

the study exhibited normal cognition (O'Bryant et al., 2008; Pinto et al., 2019) with MoCA scores > 23 (27.07 ± 1.66) and MMSE scores > 27 (28.60 ± 1.02). After screening for cognition, 3 young and 3 older adults were also excluded due to image alignment issues or excessive motion. The final sample included 78 young (20.50 ± 1.95 years old, 41 female) and 68 older adults (73.22 ± 5.96 years old, 37 female).

Episodic Memory Tasks

Episodic memory was assessed using the RAVLT (Rey 1941) and MST (Stark et al 2013), which provided measures of memory performance including recall, recognition, and mnemonic discrimination.

For the RAVLT, participants verbally recalled a series of words from a list of 15 words following five consecutive trials of recall of the same word list (i.e., immediate recall), and verbally recalled again after a 30-minute delay (i.e., delayed recall). Participants also completed a verbal recognition trial by identifying the 15 words from the original list, out of a list of 30 words.

For the MST, participants viewed 128 images of everyday objects (e.g. a rubber duck) during an active encoding phase (for more details, see Klippenstein, Stark, Stark, & Bennett, 2020), followed by a test phase where participants judged the images as "new" or "old" using a two-choice button press. To measure mnemonic discrimination, a lure discrimination index (LDI; Stark, Stevenson, Wu, Rutledge, & Stark, 2015), was calculated as proportion of correctly judging a similar image (lure) as "new", minus incorrectly judging a repeated image as "new" (hits – false alarms). A traditional recognition measure was calculated as the probability of a participant correctly judging a

repeated image as “old”, minus the probability of incorrectly judging a new image as “old”. Participants who had >20% omitted trials (2 younger and 2 older adults) or extremely poor recognition (> 2.5 SD from the mean; 2 younger and 1 older adult) in the MST were excluded and the final sample size for MST analyses was 74 young (20.58 ± 1.98 years old, 39 female) and 66 older adults (73.19 ± 6.08 years old, 36 female).

MRI Scanning Protocol

Imaging data were acquired at the UCR Center for Advanced Neuroimaging using a 3T Siemens Prisma magnetic resonance imaging (MRI; Siemens Healthineers, Malvern, PA) scanner fitted with a 32-channel receive-only head coil. For the high-resolution magnetization prepared rapid gradient-echo (MPRAGE) images, the parameters were: echo time (TE)/repetition time (TR) = 2.72/2400 ms, 208 axial slices, voxel size = 0.8×0.8×0.8 mm, and GRAPPA acceleration factor = 2. For diffusion-weighted echo-planar imaging (EPI) with reverse phase-encoding, the parameters were: TE/TR = 102/3500 ms, FOV = 212×182 mm, matrix size of 128×110, voxel size = 1.7×1.7×1.7 mm, 64 axial slices, and multiband acceleration factor = 4. Six images had no diffusion weighting (b = 0; 12 total) and remaining images had bipolar diffusion encoding gradients (b = 1500 and 3000 s/mm^2) applied in 64 orthogonal directions for each acquisition. Multi-echo data derived from a 12-echo 3D gradient recalled echo (GRE) sequences, the parameters were: TE/ΔTE/TR = 4/3/40 ms, FOV = 192×224 mm, matrix size = 192×224×96, slice thickness = 1.7 mm, and GRAPPA acceleration factor = 2.

Diffusion Data Processing

All diffusion data were pre-processed using the FMRIB Software Library (FSL; Jenkinson, Beckmann, Behrens, Woolrich, & Smith, 2012), except for the binary brain mask, which used Analysis of Functional Neuro Images (AFNI; Cox 1996). Following generation of the susceptibility off-resonance field map by FSL's topup, eddy was used to correct for distortions due to eddy-currents, susceptibility, and motion (Andersson, Skare, & Ashburner, 2003; Andersson & Sotiropoulos, 2016). Single-tensor whole brain voxel-wise images of FA and MD were generated using FSL's dtifit.

The NODDI MATLAB toolbox was used to model whole brain voxel-wise measures of restricted (or intracellular volume fraction, ICVF), hindered (or orientation dispersion index, ODI) and free (or isotropic fraction, fISO) diffusion (http://mig.cs.ucl.ac.uk/index.php; Zhang, Schneider, Wheeler-Kingshott, & Alexander, 2012). The intrinsic diffusivity assumption was set to 1.1×10^{-3} mm^2/s (Guerrero et al. 2019, Fukutomi et al., 2019, 2018), to more accurately model restricted and hindered diffusion in gray matter. To limit restricted and hindered diffusion metrics to voxels with sufficient tissue content, an inclusion mask was created by thresholding the free diffusion image to remove voxels with very high free water (> 90%).

Region of Interest Segmentations

Region of interest (ROI) segmentations were conducted independently on each participant's MPRAGE image for cortical and subcortical brain regions. Bilateral cortical and ROIs were automatically segmented using the 1 mm Harvard Oxford atlas in MNI standard space (25% threshold, Desikan et al., 2006), whereas subcortical ROIs were

segmented using the FSL's Integrated Registration and Segmentation Tool (FIRST; Patenaude, Smith, Kennedy, & Jenkinson, 2011).

For each participant, diffusion metrics were extracted separately for each segmented ROI. First, a rigid body (6 degrees of freedom; DOF) transformation with the boundary based registration (BBR; Greve & Fischl, 2009) cost function was used align each subject's b=0 diffusion image to their MPRAGE image using FLIRT, and then inverted. For subcortical ROIs, the inverted BBR transformation was then used to align FIRST segmented ROIs to diffusion space using FLIRT (12 DOF); the three-stage affine registration was used for hippocampus (as in Venkatesh et al., 2020). For cortical ROIs, each subject's MPRAGE image was aligned to 1mm MNI standard space using an affine (12 DOF) transformation. The BBR transformation was concatenated with the MNI transformation and inverted to generate a MNI to diffusion space transformation, which was used to align the cortical ROIs from the 1mm Harvard Oxford atlas to diffusion space. To ensure that each cortical ROI was limited to gray matter, each subject's gray matter segmentation from FMRIB's Automated Segmentation Tool (FAST; Y. Zhang, Brady, & Smith, 2001) was binarized and multiplied by the cortical ROIs in diffusion space. Each bilateral diffusion space-aligned ROI mask was then binarized and multiplied by the voxel-wise diffusion images before taking the average across voxels and hemispheres. For restricted and hindered diffusion measures only, the inclusion mask was multiplied prior to taking the average.

Quality control of the alignments and segmentations, which included allowing no more than a 1-2 voxel shift between alignments and checking for accuracy of the segmentations, was completed by a trained researcher and did not yield notable age differences.

Cortical Lobes

Given the numerous individual ROIs in the Harvard Oxford atlas (n = 47), cortical analyses were simplified by grouping the ROIs into four primary lobes including frontal, temporal, parietal, and occipital lobe. Lobes were grouped after aligning ROIs into diffusion space. Regions for frontal lobe included frontal pole, superior frontal gyrus, middle frontal gyrus, inferior frontal gyrus pars triangularis, inferior frontal gyrus pars opercularis, precentral gyrus, frontal medial cortex, juxtapositional lobule, subcallosal cortex, paracingulate gyrus, frontal orbital cortex, frontal operculum, cingulate gyrus anterior division, insular cortex. Regions for temporal lobe included temporal pole, temporal gyrus (auditory cortex; Fitzhugh, Hemesath, Schaefer, Baxter, & Rogalsky, 2019), parahippocampal gyrus anterior division, parahippocampal gyrus posterior division, temporal fusiform cortex-anterior division, temporal fusiform cortex-posterior division, temporal occipital fusiform, planum polare, Heschl's gyrus (primary auditory cortex; Fitzhugh et al., 2019), planum temporale (language area; Hickok, 2009). Regions for parietal lobe included postcentral gyrus, superior pariental lobule, supramarginal gyrus-anterior division, supramarginal gyrus-posterior division, angular gyrus, precuneous, parietal operculum, central operculum, cingulate gyrus posterior division. Regions for occipital lobe included lateral occipital cortex- superior division (object

recognition; Grill-Spector, Kourtzi, & Kanwisher, 2001), lateral occipital cortex-inferior division, intracalcarine cortex (primary visual cortex; Rosenthal, Andrews, Antoniades, Kennard, & Soto Correspondence, 2016), cuneal cortex, lingual gyrus, supracalcarine cortex, occipital pole, occipital fusiform

Statistical Analyses

All regression analyses were conducted using SPSS (Version 24.0; IBM, Armonk, NY, USA) and figures were generated using Prism (Version 7.0d; GraphPad Software, La Jolla California USA). For all analyses, the significance threshold was set after Bonferroni correction for multiple comparisons ($p < 0.05$ divided by number of comparisons).

Results

Age Group Differences in Memory Performance

Age group differences in RAVLT performance were largely as expected, with the older adults having lower scores compared in the young adults. For RAVLT immediate recall, results from independent sample *t*-tests demonstrated that significantly fewer words were recalled by older adults (8.53 ± 2.93) compared to young (11.24 ± 2.54), $t(144) = 5.99$, $p < 0.001$. Similarly for RAVLT delayed recall, significantly fewer words were recalled by older adults (7.88 ± 3.10) compared to the young (10.83 ± 2.82), $t(144) = 6.01$, $p < 0.001$. Lastly, for RAVLT recognition, older adults recognized significantly few words (10.04 ± 3.96) than the young adults (12.85 ± 2.53), $t(144) = 5.16$, $p < 0.001$, see Figure 1.

Age group differences in MST performance were also as expected, with older adults having lower scores than young adults for discrimination but not recognition. For LDI, results from independent sample *t*-tests demonstrated that older adults were significantly impaired at distinguishing lure images compared to young, $t(138) = 5.38$, $p < 0.001$. The age group difference in the recognition performance, $p > 0.02$, did not survive multiple comparisons correction, (five behavioral measures, $p < 0.01$).

Age Group Differences in Diffusion Measures

Age group differences in gray matter diffusion measures were observed for both DTI (FA, MD) and NODDI (restricted, hindered, and free diffusion) measures using independent sample *t*-tests. To be considered significant, age group differences needed to survive multiple comparisons correction for 40 comparisons (five measures in eight brain regions, $p < 0.0013$), see Table1.

For FA, older adults had higher values (0.22 ± 0.001) than young (0.20 ± 0.001) in most regions except in the hippocampus, which showed the opposite trend, see Table 1. For MD, older adults had lower values ($4.0 \pm 0.02 \times 10^{-4}$) compared to young ($5.0 \pm 0.02 \times 10^{-4}$) in most ROIs.

For NODDI measures, restricted diffusion significantly differed across all ROIs, with higher values in older adults (0.47 ± 0.003) compared to young (0.39 ± 0.003). Although hindered diffusion was also higher in older adults (0.40 ± 0.002) compared to young (0.39 ± 0.001), significant results were limited to frontal lobe, temporal lobe, and hippocampus. Lastly, for free diffusion older adults had higher values (0.26 ± 0.003) than young (0.19 ± 0.003) in all ROIs except globus pallidus.

Relationships Between Microstructure and Age Group

To determine the single best predictor of age among all DTI (FA, MD) and NODDI (restricted, hindered and free diffusion) measures, a forward logistic regression was run with cortical and subcortical regions entered together. Results revealed that the best predictor of age group was frontal lobe free diffusion, *Nagelkerke* $R^2 = 0.90$, $p < 0.001$, see Table 2. At the second step, putamen FA was added, *Nagelkerke* $R^2 = 1.00$, which did not significantly improve the variance explained ($p > 0.96$), however the model was significantly changed if the term was removed, $p < 0.001$. Lastly, in the third step occipital lobe hindered diffusion was added, although it did not significantly improve the variance explained ($p > 0.99$).

Relationships Between Microstructure and Memory Performance

To determine the ability of DTI (FA, MD) and NODDI (restricted, hindered and free diffusion) diffusion measures to account for variance in memory performance, forward stepwise regressions were run separately for cortical lobes and subcortical regions, for each behavioral measure. To account for the possibility that demographic variables affect results, age group, sex and education level were also entered as predictors for all stepwise regressions, see Table 3. The standardized coefficient (β) and *p*-values for each significant measure from the final model are reported below, significant results needed to survive multiple comparisons correction (five behavioral measures, $p < 0.01$).

Results for RAVLT immediate recall revealed that hippocampal restricted diffusion was a significant predictor of performance, $\beta = -0.37$, $p < 0.001$. For RAVLT delayed recall, frontal lobe free, $\beta = -0.45$, $p < 0.001$, hippocampal restricted, $\beta = -0.30$,

$p < 0.004$ and putamen free, $\beta = -0.30$, $p < 0.004$, diffusion were significant predictors of performance. For RAVLT recognition, frontal lobe free, $\beta = -0.43$, $p < 0.001$ and putamen free, $\beta = -0.32$, $p < 0.003$, diffusion were significant predictors of performance, see Table 3. For MST LDI, hippocampal hindered diffusion was the single best predictor of performance, $\beta = -0.45$, $p < 0.001$. For MST recognition, occipital lobe free, $\beta = -0.28$, $p < 0.002$, and hippocampal hindered, $\beta = -0.35$, $p < 0.001$, diffusion were significant predictors.

Lastly, relationships between sensory cortices and memory performance were assessed using separate forward stepwise regressions for RAVLT and MST measures. For RAVLT performance, auditory regions entered as predictors were primary auditory cortex (Heschl's gyrus), auditory cortex (temporal gyrus) and a language area (planum temporale). Hindered diffusion from primary auditory cortex was the best predictor of delayed memory performance independent of age group and sex, $\beta = -0.21$, $p < 0.01$ and survived multiple comparisons correction ($p < 0.017$). For MST performance, visual regions entered as predictors were primary visual cortex (intracalcarine cortex), and object recognition areas (superior and inferior divisions of lateral occipital cortex). Free diffusion from primary visual cortex was the best predictor of recognition performance $\beta = -0.30$, $p < 0.001$, and survived multiple comparisons correction ($p < 0.025$).

Testing for Age Moderating Diffusion-Memory Relationships

To test the possibility that the relationships between diffusion measures and memory performance were moderated by age group, significant predictor variables from the stepwise regressions were entered into separate linear regressions with Age Group,

Diffusion Measure and Age Group x Diffusion Measure. Regions that displayed significant associations with multiple behavioral measures (e.g. hippocampus) survived comparisons correction, select results are shown in Figure 3. There was no evidence of age group moderation; the interaction term was insignificant for all regions ($ps > 0.05$), indicating that the relationships between diffusion and memory performance were comparable between young and older adults.

Discussion

The current study examined brain wide differences in gray matter microstructure and relationships to memory performance using young and older adults. Results revealed several important findings including: (1) significant age-group differences in DTI and NODDI diffusion measures for cortical and subcortical brain regions (2) the single best predictor of age was frontal lobe free diffusion, and (3) significant relationships between NODDI measures and memory performance for recall, recognition, and mnemonic discrimination, in cortex, basal ganglia and hippocampus. Age group differences for DTI revealed generally higher FA (except in hippocampus) and lower MD in older adults compared to young, whereas all three NODDI measures were higher in older adults. The finding that the frontal lobe free water compartment was the best predictor of age was consistent with existing cognitive aging hypotheses including the free-water accumulation model (Chad et al., 2018b) and frontal-lobe hypothesis (West, 1996). Lastly, the significant relationships to memory performance replicated and extended the existing literature; the hippocampal findings for both RAVLT and MST performance were in line with previous work (Radhakrishnan et al., 2020; Venkatesh et al., 2020), and

cortical findings extend previous fMRI (Fan, Yamins, & Turk-Browne, 2018; Rosenthal et al., 2016) results in young adults to gray matter microstructure in young and older adults. The current study improves understanding of gray matter microstructure and relationships to memory performance while extending our previously reported finding, that NODDI measures are more sensitive to age and memory performance compared to DTI (Venkatesh et al., 2020), in regions beyond the hippocampus.

Compared to DTI measures, age group differences in NODDI measures were more sensitive to differences in cortical lobes and provided insighted into how tissue and non-tissue compartments differed between young and older adults. Although both diffusion approaches were sensitive to age group difference in subcortical regions, NODDI measures also captured differences in cortical regions (e.g., older adults had significantly higher restricted and free diffusion in occipital lobe). With regard to relationships between DTI and NODDI measures, at least one paper has shown a negative association between restricted diffusion and MD in gray matter (Fukutomi et al., 2018b), which is consistent with the current study, where older adults displayed higher restricted diffusion and lower MD compared to young. Higher hippocampal hindered diffusion in older adults is consistent with two previous studies (Nazeri et al., 2015; Venkatesh et al., 2020), although, the results for the cortical lobes conflicted with Nazeri et al., which showed an age-related decrease in hindered diffusion within cortical regions (2015). Perhaps hindered diffusion in cortical regions is more affected by methodological (b-values, intrinsic diffusivity values) differences between studies.

Despite this, the finding that a tissue compartment (restricted diffusion) was sensitive to age group differences for all ROIs may suggest that NODDI is more sensitive to a unique feature of gray matter microstructure, that DTI could not capture.

Results from the forward logistic regression suggest that frontal lobe free water is the single best predictor of age and is consistent with existing hypotheses in cognitive aging. DTI (FA, MD) and NODDI (restricted, hindered and free diffusion) measures for all eight gray matter regions were entered into the model, and the top two predictors were frontal lobe free water and putamen FA. This is a significant finding, as it supports both the free water accumulation model (Chad et al., 2018b; Ofori et al., 2015; Pasternak et al., 2009; Simon & Iliff, 2016) and frontal lobe hypothesis (Greenwood, 2000; Raz et al., 2005; Resnick et al., 2003; West, 1996) in gray matter. Age-related accumulation of free water is presumably due to an increase in age-related inflammatory factors, which dysregulate the glial (astrocyte) networks responsible for managing CSF (Fukuda & Badaut, 2012; Simon & Iliff, 2016). An age-related increase in free water has been previously reported in white matter tracts and hippocampal gray matter and found to be highly sensitive to age (Chad et al., 2018b; Venkatesh et al., 2020) and cognition (Gullett et al., 2020; Maillard et al., 2019) in older adults. Consistent with the idea that other brain regions are also sensitive to age (Greenwood, 2000), we do find that putamen and occipital lobe were also significant predictors of age in the model. These results suggest that while the effects of age are seen in multiple gray matter regions, the frontal cortex may be most affected by age.

Within the hippocampus, the relationships between microstructure and memory performance were consistent with results from the existing literature, while extending knowledge of how specific tissue features relate to recall and recognition and mnemonic discrimination. Hippocampal tissue compartments (restricted and hindered diffusion) were found to be the best predictors of memory performance, which is similar to previous findings in hippocampus (Radhakrishnan et al., 2020; Venkatesh et al., 2020). Importantly, we extend this literature by showing that NODDI measures have task selectivity for memory performance (restricted diffusion for RAVLT, hindered diffusion for MST), which suggests that different tissue features within hippocampus support different measures of memory performance (e.g., delayed recall vs. mnemonic discrimination). One reason these measures may be negatively associated with performance is that NODDI restricted and hindered diffusion measures may partially reflect inflammation related astrocytic swelling (Badaut et al., 2011; Debacker et al., 2020) and microglial proliferation (Yi et al., 2019), with higher levels associated with poorer memory performance. Additionally, since mnemonic discrimination is thought to rely on pattern separation supported by granule cell dendrites (Chavlis et al., 2017), our results would suggest that the hippocampal hindered diffusion is also partially sensitive to a pattern where greater cell complexity is associated with poorer mnemonic discrimination. These results emphasize the need for studies which use diffusion imaging in conjunction with histology or other neuroimaging techniques (e.g., quantitative relaxometry, positron emission tomography) to parse out the relative contributions of

each microstructural feature to the NODDI measures, since the restricted and hindered compartments likely capture the contributions of both glia and neurons.

In contrast to the hippocampus, relationships to performance in cortical regions and putamen identified the non-tissue compartment (free water) as the best predictor of memory performance. The findings in cortex are consistent with previous studies which showed similar relationships between free water and cognition in cortical white matter (Gullett et al., 2020; Maillard et al., 2019). For putamen, although literature in aging (Franco et al., 2020) and Parkinson's Disease (PD; Burciu et al., 2017; Ofori et al., 2015) have also shown increases in putamen free water (Burciu et al., 2017; Franco et al., 2020; Ofori et al., 2015), we are the first to report significant relationships between putamen free water and memory performance in young and older adults. This supports a role for basal ganglia subregions in memory performance and additional work is needed identify how this may differ or complemental cortical and hippocampal networks. Lastly, the relationships to performance in primary visual and auditory cortices for RAVLT and MST extend previously reported findings from fMRI studies (Fan et al., 2018; Goveas et al., 2011; Rosenthal et al., 2016; Sala-Llonch et al., 2014) in young adults. In particular, the relationship between primary visual cortex and recognition memory in both young and older adults suggests a strong concordance between fMRI (Fan et al., 2018; Rosenthal et al., 2016) and diffusion imaging.

Overall, the current study establishes the utility of NODDI measures to capture age group differences in gray matter microstructure and relationships to memory performance. This approach lends support to existing hypotheses in cognitive aging,

while extending findings from young adults in fMRI studies. Importantly, the current study has begun to parse out the specific roles for microstructural features for explains relationships in age and facets of memory performance. The overall pattern suggests that tissue and non-tissue compartments regionally vary in relationships to age and memory such that tissue compartments are well suited in hippocampus for associations with multiple memory measures, but that free diffusion is better suited in other gray matter regions (e.g., frontal lobe, putamen) for capturing differences in age and memory. Similar pattens of results between diffusion imaging and fMRI for cortical findings suggest a strong concordance between MRI techniques, although the utility of gray matter free diffusion for assessing cognition and brain aging suggests that future studies using older adults would benefit by including a measure of free water. Although more studies are needed to fully understand the contributions of gray matter microstructure to memory decline, the current study provides a foundation of knowledge for brain wide differences in microstructure and relationships to age and memory performance.

Table 3 Age group differences in diffusion measures

Gray Matter Region	*t*	Young	Older
FA			
Frontal Lobe	7.58*	0.16 ± 0.01	0.17 ± 0.01
Temporal Lobe	-5.3	0.18 ± 0.01	0.17 ± 0.01
Parietal Lobe	4.50*	0.17 ± 0.01	0.18 ± 0.01
Occipital Lobe	3.02	0.14 ± 0.01	0.15 ± 0.01
Hippocampus	8.06*	0.18 ± 0.01	0.17 ± 0.01
Caudate	7.13*	0.19 ± 0.02	0.22 ± 0.02
Putamen	18.89*	0.21 ± 0.01	0.27 ± 0.03
Globus Pallidus	6.76*	0.37 ± 0.04	0.42 ± 0.05
MD ($\times 10^{-4} mm^2/s$)			
Frontal Lobe	-7.41*	6.01 ± 0.15	5.87 ± 0.17
Temporal Lobe	-7.41*	5.65 ± 0.19	5.43 ± 0.17
Parietal Lobe	-3.36	5.92 ± 0.13	5.84 ± 0.14
Occipital Lobe	-1.60	5.58 ± 0.33	5.51 ± 0.33
Hippocampus	-6.80*	5.42 ± 0.20	5.19 ± 0.20
Caudate	-9.66*	5.13 ± 0.19	4.74 ± 0.29
Putamen	-16.19*	4.80 ± 0.22	3.96 ± 0.39
Globus Pallidus	-6.28*	2.91 ± 0.26	2.57 ± 0.39
Restricted (ICVF)			
Frontal Lobe	16.83*	0.31 ± 0.02	0.26 ± 0.02
Temporal Lobe	9.18*	0.34 ± 0.03	0.30 ± 0.03
Parietal Lobe	12.63*	0.30 ± 0.02	0.26 ± 0.02
Occipital Lobe	6.35*	0.27 ± 0.03	0.24 ± 0.03
Hippocampus	8.15*	0.44 ± 0.05	0.37 ± 0.04
Caudate	13.16*	0.50 ± 0.07	0.38 ± 0.04
Putamen	16.49*	0.63 ± 0.10	0.41 ± 0.06
Globus Pallidus	6.25*	0.93 ± 0.04	0.88 ± 0.04
Hindered (ODI)			
Frontal Lobe	4.54*	0.39 ± 0.02	0.37 ± 0.02
Temporal Lobe	4.96*	0.34 ± 0.03	0.30 ± 0.03
Parietal Lobe	0.30	0.36 ± 0.01	0.36 ± 0.01
Occipital Lobe	-1.60	0.36 ± 0.03	0.36 ± 0.03
Hippocampus	8.05*	0.44 ± 0.03	0.39 ± 0.02
Caudate	1.47	0.42 ± 0.03	0.41 ± 0.02
Putamen	0.08	0.43 ± 0.03	0.43 ± 0.02
Globus Pallidus	0.32	0.43 ± 0.04	0.43 ± 0.03
Free (fISO)			
Frontal Lobe	19.41*	0.22 ± 0.03	0.13 ± 0.02
Temporal Lobe	15.18*	0.22 ± 0.03	0.16 ± 0.02
Parietal Lobe	18.84*	0.22 ± 0.03	0.13 ± 0.03
Occipital Lobe	15.47*	0.24 ± 0.04	0.14 ± 0.03
Hippocampus	8.05*	0.32 ± 0.04	0.27 ± 0.04
Caudate	14.79*	0.31 ± 0.07	0.17 ± 0.04
Putamen	12.85*	0.29 ± 0.06	0.17 ± 0.05
Globus Pallidus	0.01	0.30 ± 0.07	0.32 ± 0.04

Note: The *t* statistic and M ± SD are presented for NODDI measures. Asterisks (*) denotes significant effects at $P < 0.0013$ (Bonferroni corrected for 40 total diffusion measures)

Figure 6

Age group differences in RAVLT and MST performance

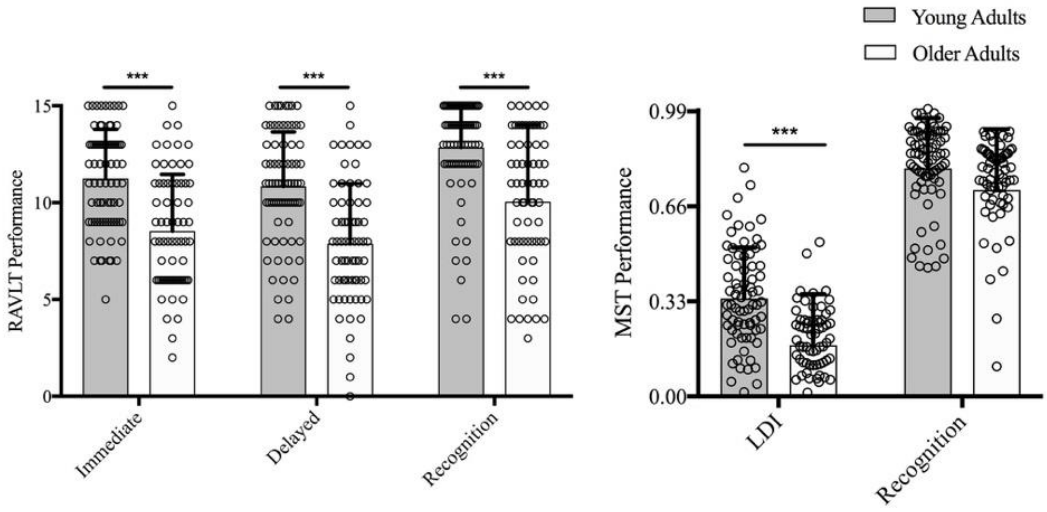

Note. *** = $p < 0.001$

Table 4

Forward (LR) logistic regression analyses performed with all diffusion measures predicting Age Group as the outcome variable.

Model	Variable	***B***	***S.E.***	**Wald**	***Sig.***	**Negelkerke R^2**
1	Frontal Lobe Free	127.94	26.57	23.18	<0.001	0.90
2	Frontal Lobe Free	1656.58	44100.16	0.001	<0.001	1.00
	Putamen FA	5694.38	150864.78	0.001	<0.001	
3	Occipital lobe Hindered	-262.38	38484.09	<0.001	0.998	1.00
	Frontal Lobe Free	1181.332	43687.95	0.001	<0.001	
	Putamen FA	3797.638	35056.41	0.001	<0.001	

Predicted variable: Age Group, B = Intercept, S.E.= Standard Error, Wald = Wald chi-square test

Sig. = Significance of model change if term is removed

Table 5

Forward stepwise regressions assess the ability of diffusion measures to account for RAVLT and MST memory performance. Final models shown.

Cortical Regions	***β***	***p***	***Model R^2***	***F***	**Model *p***
Age Group	-0.45	<0.001			
Sex	0.23	0.001	0.28	18.34	<0.001
Parietal Lobe Hindered	-0.16	0.02			
Subcortical Regions					
Hippocampus Restricted	-0.37	<0.001*	0.29	29.31	<0.001
Age Group	-0.24	0.005			
Dependent variable: RAVLT Immediate Recall					
Cortical Regions					
Frontal Lobe Free	-0.46	<0.001*	0.27	26.31	<0.001
Sex	0.22	0.002			
Subcortical Regions					
Hippocampus Restricted	-0.30	0.003*	0.31	32.08	<0.001
Putamen Free	-0.30	0.003*			
Dependent variable: RAVLT Delayed Recall					
Cortical Regions					
Frontal Lobe Free	-0.43	<0.001*	0.22	20.31	<0.001
Sex	0.18	0.02			
Subcortical Regions					
Putamen Free	-0.32	0.002*	0.26	24.68	<0.001
Hippocampus Hindered	-0.22	0.04			
Dependent variable: RAVLT Recognition					
Cortical Regions	***β***	***p***	***Model R^2***	***F***	**Model *p***
Frontal Lobe Free	-0.20	0.17			
Frontal Lobe FA	0.20	0.03			
Sex	0.25	< 0.01	0.31	12.07	<0.001
Age Group	-0.35	0.02			
Temporal Lobe FA	0.19	0.02			
Subcortical Regions					
Hippocampus ODI	-0.45	<0.001*	0.20	34.89	<0.001
Dependent variable: Lure Discrimination Index					
Cortical Regions					
Occipital Lobe Free	-0.28	0.001*	0.13	9.88	<0.001
Sex	0.18	0.03			
Subcortical Regions					
Hippocampus Hindered	-0.35	<0.001*	0.13	10.12	<0.001
Putamen Hindered	0.18	0.03			
Dependent variable: MST Recognition					

Note. DTI and NODDI measures along with Age Group, Sex and Education were entered as predictor variables. β = Standardized coefficient, (*) denotes significant brain regions that survive Bonferroni correction for five behavioral measures, $p < 0.01$.

Figure 7
Relationships between diffusion measures and RAVLT and MST memory performance across regions

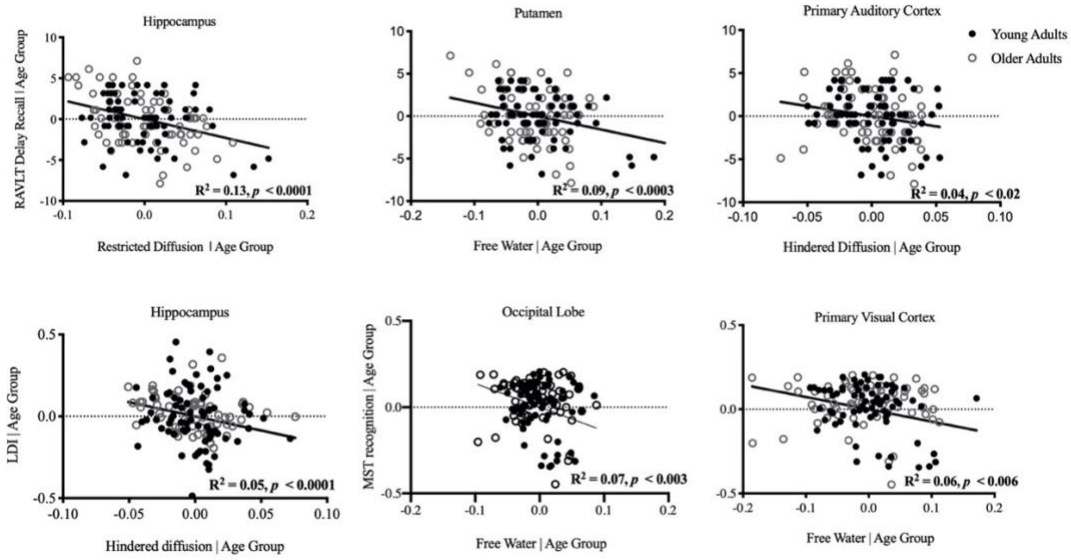

References

Andersson, J. L. R., Skare, S., & Ashburner, J. (2003). How to correct susceptibility distortions in spin-echo echo-planar images: application to diffusion tensor imaging. *NeuroImage*, *20*(2), 870–888. https://doi.org/10.1016/S1053-8119(03)00336-7

Andersson, J. L. R., & Sotiropoulos, S. N. (2016). An integrated approach to correction for off-resonance effects and subject movement in diffusion MR imaging. *Neuroimage*, *125*, 1063. https://doi.org/10.1016/J.NEUROIMAGE.2015.10.019

Badaut, J., Ashwal, S., Adami, A., Tone, B., Recker, R., Spagnoli, D., … Obenaus, A. (2011). Brain water mobility decreases after astrocytic aquaporin-4 inhibition using RNA interference. *Journal of Cerebral Blood Flow and Metabolism : Official Journal of the International Society of Cerebral Blood Flow and Metabolism*, *31*(3), 819–831. https://doi.org/10.1038/jcbfm.2010.163

Beach, T. G., Walker, R., & McGeer, E. G. (1989). Patterns of gliosis in alzheimer's disease and aging cerebrum. *Glia*, *2*(6), 420–436. https://doi.org/10.1002/glia.440020605

Bennett, I. J., Madden, D. J., Vaidya, C. J., Howard, D. V., & Howard, J. H. (2010). Age-related differences in multiple measures of white matter integrity: A diffusion tensor imaging study of healthy aging. *Human Brain Mapping*, *31*(3), 378–390. https://doi.org/10.1002/hbm.20872

Bhagat, Y. A., & Beaulieu, C. (2004). Diffusion anisotropy in subcortical white matter and cortical gray matter: Changes with aging and the role of CSF-suppression. *Journal of Magnetic Resonance Imaging*, *20*(2), 216–227. https://doi.org/10.1002/jmri.20102

Burciu, R. G., Ofori, E., Archer, D. B., Wu, S. S., Pasternak, O., McFarland, N. R., … Vaillancourt, D. E. (2017). Progression marker of Parkinson's disease: A 4-year multi-site imaging study. *Brain*, *140*(8), 2183–2192. https://doi.org/10.1093/brain/awx146

Càmara, E., Bodammer, N., Rodríguez-Fornells, A., & Tempelmann, C. (2007). Age-related water diffusion changes in human brain: A voxel-based approach. *NeuroImage*, *34*(4), 1588–1599. https://doi.org/10.1016/j.neuroimage.2006.09.045

Carlesimo, G. A., Cherubini, A., Caltagirone, C., & Spalletta, G. (2010). Hippocampal mean diffusivity and memory in healthy elderly individuals: A cross-sectional study. *Neurology*, *74*(3), 194–200. https://doi.org/10.1212/WNL.0b013e3181cb3e39

Chad, J. A., Pasternak, O., Salat, D. H., & Chen, J. J. (2018). Re-examining age-related differences in white matter microstructure with free-water corrected diffusion tensor imaging. *Neurobiology of Aging*, *71*, 161–170. https://doi.org/10.1016/j.neurobiolaging.2018.07.018

Chavlis, S., Petrantonakis, P. C., & Poirazi, P. (2017). Dendrites of dentate gyrus granule cells contribute to pattern separation by controlling sparsity. *Hippocampus*, *27*(1), 89–110. https://doi.org/10.1002/hipo.22675

Cherubini, A., Péran, P., Caltagirone, C., Sabatini, U., & Spalletta, G. (2009). Aging of subcortical nuclei: Microstructural, mineralization and atrophy modifications measured in vivo using MRI. *NeuroImage*, *48*(1), 29–36. https://doi.org/10.1016/j.neuroimage.2009.06.035

Colgan, N., Siow, B., O 'callaghan, J. M., Harrison, I. F., Wells, J. A., Holmes, H. E., … Lythgoe, M. F. (2016). Application of neurite orientation dispersion and density imaging (NODDI) to a tau pathology model of Alzheimer's disease. *NeuroImage*, *125*, 739–744. https://doi.org/10.1016/j.neuroimage.2015.10.043

Craik, F. I. M. (1986). A functional account of age differences in memory. *Memory, Attention, and Aging: Selected Works of Fergus I. M. Craik*, (January 1986), 147–157. https://doi.org/10.4324/9781315440446

Danckert, S. L., & Craik, F. I. M. (2013). Does aging affect recall more than recognition memory? *Psychology and Aging*, *28*(4), 902–909. https://doi.org/10.1037/a0033263

Debacker, C., Djemai, B., Ciobanu, L., Tsurugizawa, T., & Bihan, D. Le. (2020). Diffusion MRI reveals in vivo and non-invasively changes in astrocyte function induced by an aquaporin-4 inhibitor. *PLoS ONE*, *15*(5). https://doi.org/10.1371/journal.pone.0229702

Dempster, F. N. (1992). The rise and fall of the inhibitory mechanism: Toward a unified theory of cognitive development and aging. *Developmental Review*, *12*(1), 45–75. https://doi.org/10.1016/0273-2297(92)90003-K

Den Heijer, T., der Lijn, F. van, Vernooij, M. W., de Groot, M., Koudstaal, P. J., der Lugt, A. van, … Breteler, M. M. B. (2012). Structural and diffusion MRI measures of the hippocampus and memory performance. *NeuroImage*, *63*(4), 1782–1789. https://doi.org/10.1016/j.neuroimage.2012.08.067

Desikan, R. S., Ségonne, F., Fischl, B., Quinn, B. T., Dickerson, B. C., Blacker, D., … Killiany, R. J. (2006). An automated labeling system for subdividing the human cerebral cortex on MRI scans into gyral based regions of interest. *NeuroImage*, *31*(3), 968–980. https://doi.org/10.1016/j.neuroimage.2006.01.021

Fan, J. E., Yamins, D. L. K., & Turk-Browne, N. B. (2018). Common Object Representations for Visual Production and Recognition. *Cognitive Science, 42*(8), 2670–2698. https://doi.org/10.1111/cogs.12676

Fitzhugh, M. C., Hemesath, A., Schaefer, S. Y., Baxter, L. C., & Rogalsky, C. (2019). Functional Connectivity of Heschl's Gyrus Associated With Age-Related Hearing Loss: A Resting-State fMRI Study. *Frontiers in Psychology*, *10*. https://doi.org/10.3389/fpsyg.2019.02485

Folstein, M. F., Folstein, S. E., & McHugh, P. R. (1975). "Mini-mental state". A practical method for grading the cognitive state of patients for the clinician. *Journal of Psychiatric Research, 12*(3), 189–198. https://doi.org/10.1016/0022-3956(75)90026-6

Franco, C. Y., Petok, J. R., Langley, J., Hu, X., & Bennett, I. J. (2020). Implicit associative learning relates to basal ganglia gray matter microstructure in young and older adults. *Behavioural Brain Research*, *397*. https://doi.org/10.1016/j.bbr.2020.112950

Fukuda, A. M., & Badaut, J. (2012, December 27). Aquaporin 4: A player in cerebral edema and neuroinflammation. *Journal of Neuroinflammation*. BioMed Central. https://doi.org/10.1186/1742-2094-9-279

Fukutomi, H., Glasser, M. F., Murata, K., Akasaka, T., Fujimoto, K., Yamamoto, T., … Hayashi, T. (2019). Diffusion Tensor Model links to Neurite Orientation Dispersion and Density Imaging at high b-value in Cerebral Cortical Gray Matter. *Scientific Reports, 9*(1), 12246. https://doi.org/10.1038/s41598-019-48671-7

Fukutomi, H., Glasser, M. F., Zhang, H., Autio, J. A., Coalson, T. S., Okada, T., … Hayashi, T. (2018a). Neurite imaging reveals microstructural variations in human cerebral cortical gray matter. *NeuroImage, 182*, 488–499. https://doi.org/10.1016/J.NEUROIMAGE.2018.02.017

Fukutomi, H., Glasser, M. F., Zhang, H., Autio, J. A., Coalson, T. S., Okada, T., … Hayashi, T. (2018b). Neurite imaging reveals microstructural variations in human cerebral cortical gray matter. *NeuroImage, 182*, 488–499. https://doi.org/10.1016/j.neuroimage.2018.02.017

Gatto, R. G., Mustafi, S. M., Amin, M. Y., Mareci, T. H., Wu, Y. C., & Magin, R. L. (2018). Neurite orientation dispersion and density imaging can detect presymptomatic axonal degeneration in the spinal cord of ALS mice. *Functional Neurology, 33*(3), 155–163. https://doi.org/10.11138/FNeur/2018.33.3.155

Goveas, J., Xie, C., Wu, Z., Douglas Ward, B., Li, W., Franczak, M. B., … Li, S. J. (2011). Neural correlates of the interactive relationship between memory deficits and depressive symptoms in nondemented elderly: Resting fMRI study. *Behavioural Brain Research*, *219*(2), 205–212. https://doi.org/10.1016/j.bbr.2011.01.008

Greenwood, P. M. (2000). The frontal aging hypothesis evaluated. *Journal of the International Neuropsychological Society*, *6*(6), 705–726. https://doi.org/10.1017/S1355617700666092

Greve, D. N., & Fischl, B. (2009). Accurate and robust brain image alignment using boundary-based registration. *NeuroImage*, *48*, 63–72. https://doi.org/10.1016/j.neuroimage.2009.06.060

Grieve, S. M., Clark, C. R., Williams, L. M., Peduto, A. J., & Gordon, E. (2005). Preservation of limbic and paralimbic structures in aging. *Human Brain Mapping*, *25*(4), 391–401. https://doi.org/10.1002/hbm.20115

Grill-Spector, K., Kourtzi, Z., & Kanwisher, N. (2001). The lateral occipital complex and its role in object recognition. In *Vision Research* (Vol. 41, pp. 1409–1422). Pergamon. https://doi.org/10.1016/S0042-6989(01)00073-6

Grussu, F., Schneider, T., Tur, C., Yates, R. L., Tachrount, M., Ianuş, A., … Gandini Wheeler-Kingshott, C. A. M. (2017). Neurite dispersion: a new marker of multiple sclerosis spinal cord pathology? *Annals of Clinical and Translational Neurology*, *4*(9), 663–679. https://doi.org/10.1002/acn3.445

Guerrero, J. M., Adluru, N., Bendlin, B. B., Goldsmith, H. H., Schaefer, S. M., Davidson, R. J., … Alexander, A. L. (2019). Optimizing the intrinsic parallel diffusivity in NODDI: An extensive empirical evaluation. *PLOS ONE*, *14*(9), e0217118. https://doi.org/10.1371/journal.pone.0217118

Gullett, J. M., O'Shea, A., Lamb, D. G., Porges, E. C., O'Shea, D. M., Pasternak, O., … Woods, A. J. (2020). The association of white matter free water with cognition in older adults. *NeuroImage*, *219*. https://doi.org/10.1016/j.neuroimage.2020.117040

Hickok, G. (2009, September). The functional neuroanatomy of language. *Physics of Life Reviews*. NIH Public Access. https://doi.org/10.1016/j.plrev.2009.06.001

Jenkinson, M., Beckmann, C. F., Behrens, T. E. J., Woolrich, M. W., & Smith, S. M. (2012). FSL. *NeuroImage*, *62*(2), 782–790. https://doi.org/10.1016/J.NEUROIMAGE.2011.09.015

Klippenstein, J. L., Stark, S. M., Stark, C. E. L., & Bennett, I. J. (2020). Neural substrates of mnemonic discrimination: A whole-brain fMRI investigation. https://doi.org/10.1002/brb3.1560

Kojima, K., April, C., Canasto-Chibuque, C., Chen, X., Deshmukh, M., Venkatesh, A., … Hoshida, Y. (2014). Transcriptome profiling of archived sectioned formalin-fixed paraffin-embedded (AS-FFPE) tissue for disease classification. *PloS One*, *9*(1), e86961. https://doi.org/10.1371/journal.pone.0086961

Liu, X., Erikson, C., & Brun, A. (1996). Cortical Synaptic Changes and Gliosis in Normal Aging, Alzheimer's Disease and Frontal Lobe Degeneration. *Dementia and Geriatric Cognitive Disorders*, *7*(3), 128–134. https://doi.org/10.1159/000106867

Madden, D. J., Bennett, I. J., Burzynska, A., Potter, G. G., Chen, N., & Song, A. W. (2012). Diffusion tensor imaging of cerebral white matter integrity in cognitive aging. *Biochimica et Biophysica Acta (BBA) - Molecular Basis of Disease*, *1822*(3), 386–400. https://doi.org/10.1016/j.bbadis.2011.08.003

Maillard, P., Fletcher, E., Singh, B., Martinez, O., Johnson, D. K., Olichney, J. M., … DeCarli, C. (2019). Cerebral white matter free water: A sensitive biomarker of cognition and function. *Neurology*, 10.1212/WNL.0000000000007449. https://doi.org/10.1212/WNL.0000000000007449

Mao, J., Zeng, W., Zhang, Q., Yang, Z., Yan, X., Zhang, H., … Shen, J. (2020). Differentiation between high-grade gliomas and solitary brain metastases: a comparison of five diffusion-weighted MRI models. *BMC Medical Imaging*, *20*(1), 124. https://doi.org/10.1186/s12880-020-00524-w

Mori, S., & Zhang, J. (2006, September 7). Principles of Diffusion Tensor Imaging and Its Applications to Basic Neuroscience Research. *Neuron*. Cell Press. https://doi.org/10.1016/j.neuron.2006.08.012

Nash, M. I., Cooper, |, Hodges, B., Muncy, N. M., Brock Kirwan, | C, & Kirwan, C. B. (2021). Pattern separation beyond the hippocampus: A high-resolution whole-brain investigation of mnemonic discrimination in healthy adults. https://doi.org/10.1002/hipo.23299

Nasreddine, Z. S., Phillips, N. A., BÃ©dirian, V., Charbonneau, S., Whitehead, V., Collin, I., … Chertkow, H. (2005). The Montreal Cognitive Assessment, MoCA: A Brief Screening Tool For Mild Cognitive Impairment. *Journal of the American Geriatrics Society*, *53*(4), 695–699. https://doi.org/10.1111/j.1532-5415.2005.53221.x

Nazeri, A., Chakravart, M., Rotenberg, D. J., Rajji, T. K., Rathi, X., Michailovich, O. V., & Voineskos, A. N. (2015). Functional consequences of neurite orientation dispersion and density in humans across the adult lifespan. *Journal of Neuroscience*, *35*(4), 1753–1762. https://doi.org/10.1523/JNEUROSCI.3979-14.2015

O'Bryant, S. E., Humphreys, J. D., Smith, G. E., Ivnik, R. J., Graff-Radford, N. R., Petersen, R. C., & Lucas, J. A. (2008). *Detecting dementia with the mini-mental state examination in highly educated individuals*. *Archives of Neurology* (Vol. 65). https://doi.org/10.1001/archneur.65.7.963

Ofori, E., Pasternak, O., Planetta, P., Burciu, R., Snyder, A., Febo, M., … Vaillancourt, D. (2015). Increased free-water in the substantia nigra of Parkinson's disease: a single-site and multi-site study. *Neurobiol Aging*, *36*(2), 1097–1104. https://doi.org/10.1016/j.neurobiolaging.2014.10.029

Pasternak, O., Sochen, N., Gur, Y., Intrator, N., & Assaf, Y. (2009). Free water elimination and mapping from diffusion MRI. *Magnetic Resonance in Medicine*, *62*(3), 717–730. https://doi.org/10.1002/mrm.22055

Pendlebury, S. T., Welch, S. J. V, Cuthbertson, F. C., Mariz, J., Mehta, Z., & Rothwell, P. M. (2017). Telephone assessment of cognition after TIA and stroke : TICSm and telephone MoCA vs face-to-face MoCA and neuropsychological battery. *Stroke*, *44*(1), 227–229. https://doi.org/10.1161/STROKEAHA.112.673384.Telephone

Pereira, J. B., Valls-Pedret, C., Ros, E., Palacios, E., Falcón, C., Bargalló, N., … Junque, C. (2014). Regional vulnerability of hippocampal subfields to aging measured by structural and diffusion MRI. *Hippocampus*, *24*(4), 403–414. https://doi.org/10.1002/hipo.22234

Pfefferbaum, A., Adalsteinsson, E., Rohlfing, T., & Sullivan, E. V. (2010). Diffusion tensor imaging of deep gray matter brain structures: Effects of age and iron concentration. *Neurobiology of Aging*, *31*(3), 482–493. https://doi.org/10.1016/j.neurobiolaging.2008.04.013

Pfefferbaum, A., Adalsteinsson, E., & Sullivan, E. V. (2005). Frontal circuitry degradation marks healthy adult aging: Evidence from diffusion tensor imaging. *NeuroImage*, *26*(3), 891–899. https://doi.org/10.1016/j.neuroimage.2005.02.034

Pinto, T. C. C., Santos, M. S. P., Machado, L., Bulgacov, T. M., Rodrigues-Junior, A. L., Silva, G. A., … Sougey, E. B. (2019). Optimal Cutoff Scores for Dementia and Mild Cognitive Impairment in the Brazilian Version of the Montreal Cognitive Assessment among the Elderly. *Dementia and Geriatric Cognitive Disorders Extra*, *9*(1), 44–52. https://doi.org/10.1159/000495562

Radhakrishnan, H., Stark, S. M., & Stark, C. E. L. (2020). Microstructural Alterations in Hippocampal Subfields Mediate Age-Related Memory Decline in Humans. *Frontiers in Aging Neuroscience*, *12*. https://doi.org/10.3389/fnagi.2020.00094

Rathi, Y., Pasternak, O., Savadjiev, P., Michailovich, O., Bouix, S., Kubicki, M., … Shenton, M. E. (2014). Gray matter alterations in early aging: A diffusion magnetic resonance imaging study. *Human Brain Mapping*, *35*(8), 3841–3856. https://doi.org/10.1002/hbm.22441

Raz, N., Lindenberger, U., Rodrigue, K. M., Kennedy, K. M., Head, D., Williamson, A., … Acker, J. D. (2005). Regional brain changes in aging healthy adults: General trends, individual differences and modifiers. *Cerebral Cortex*, *15*(11), 1676–1689. https://doi.org/10.1093/cercor/bhi044

Resnick, S. M., Pham, D. L., Kraut, M. A., Zonderman, A. B., & Davatzikos, C. (2003). *Longitudinal Magnetic Resonance Imaging Studies of Older Adults: A Shrinking Brain*.

Rey, A. (1941). L'examen psychologique dans les cas d'encéphalopathie traumatique. https://doi.org/1943-03814-001

Rhodes, S., Greene, N. R., & Naveh-Benjamin, M. (2019, October 1). Age-related differences in recall and recognition: a meta-analysis. *Psychonomic Bulletin and Review*. Springer New York LLC. https://doi.org/10.3758/s13423-019-01649-y

Rosenthal, C. R., Andrews, S. K., Antoniades, C. A., Kennard, C., & Soto Correspondence, D. (2016). Learning and Recognition of a Non-conscious Sequence of Events in Human Primary Visual Cortex. *Current Biology*, *26*, 834–841. https://doi.org/10.1016/j.cub.2016.01.040

Sala-Llonch, R., Junqué, C., Arenaza-Urquijo, E. M., Vidal-Piñeiro, D., Valls-Pedret, C., Palacios, E. M., … Bartrés-Faz, D. (2014). Changes in whole-brain functional networks and memory performance in aging. *Neurobiology of Aging*, *35*(10), 2193–2202. https://doi.org/10.1016/j.neurobiolaging.2014.04.007

Simon, M. J., & Iliff, J. J. (2016, March 1). Regulation of cerebrospinal fluid (CSF) flow in neurodegenerative, neurovascular and neuroinflammatory disease. *Biochimica et Biophysica Acta - Molecular Basis of Disease*. Elsevier. https://doi.org/10.1016/j.bbadis.2015.10.014

Stark, S. M., & Stark, C. E. L. (2017). Age-related deficits in the mnemonic similarity task for objects and scenes. *Behavioural Brain Research*, *333*, 109–117. https://doi.org/10.1016/J.BBR.2017.06.049

Stark, S. M., Stevenson, R., Wu, C., Rutledge, S., & Stark, C. E. L. (2015). STABILITY OF AGE-RELATED DEFICITS IN THE MNEMONIC SIMILARITY TASK ACROSS TASK VARIATIONS. *Behavioral Neuroscience*, *4*(5), 547–566. https://doi.org/10.1002/wrna.1178.Alternative

Stark, S. M., Yassa, M. A., Lacy, J. W., & Stark, C. E. L. (2013). A task to assess behavioral pattern separation (BPS) in humans: Data from healthy aging and mild cognitive impairment. *Neuropsychologia*, *51*(12), 2442–2449. https://doi.org/10.1016/j.neuropsychologia.2012.12.014

Venkatesh, A., Stark, S. M., Stark, C. E. L., & Bennett, I. J. (2020). Age- and memory-related differences in hippocampal gray matter integrity are better captured by NODDI compared to single-tensor diffusion imaging. *Neurobiology of Aging*, *96*, 12–21. https://doi.org/10.1016/j.neurobiolaging.2020.08.004

Wais, P. E., Jahanikia, S., Steiner, D., Stark, C. E. L., & Gazzaley, A. (2017). Retrieval of high-fidelity memory arises from distributed cortical networks. *NeuroImage*, *149*, 178–189. https://doi.org/10.1016/j.neuroimage.2017.01.062

West, R. L. (1996). An application of prefrontal cortex function theory to cognitive aging. *Psychological Bulletin*, *120*(2), 272–292. https://doi.org/10.1037/0033-2909.120.2.272

Yi, S. Y., Barnett, B. R., Torres-Velázquez, M., Zhang, Y., Hurley, S. A., Rowley, P. A., … Yu, J. P. J. (2019). Detecting microglial density with quantitative multi-compartment diffusion MRI. *Frontiers in Neuroscience*. https://doi.org/10.3389/fnins.2019.00081

Zhang, H., Schneider, T., Wheeler-Kingshott, C. A., & Alexander, D. C. (2012). NODDI: Practical in vivo neurite orientation dispersion and density imaging of the human brain. *NeuroImage*, *61*(4), 1000–1016. https://doi.org/10.1016/j.neuroimage.2012.03.072

Zhang, Y., Brady, M., & Smith, S. (2001). Segmentation of brain MR images through a hidden Markov random field model and the expectation-maximization algorithm. *IEEE Transactions on Medical Imaging*, *20*(1), 45–57. https://doi.org/10.1109/42.906424

Chapter 3: Neuroimaging Measures of Iron and Gliosis Explain Memory Performance

Abstract

Evidence from animal and histological studies have indicated that accumulation of iron in the brain results in reactive gliosis contributes to cognitive deficits. Building on this, the current study sought to examine the effects of iron on microstructure and memory performance *in vivo* using magnetic resonance imaging (MRI) techniques such as quantitative relaxometry and multi-compartment diffusion imaging in 35 young (21.06 ± 2.18 years) and 28 older (72.58 ± 6.47 years) adults. Replicating past work, results revealed age-related increases in iron content (R_2^*) and diffusion and decreases in memory performance. Independent of age group, iron content was significantly related to restricted (intracellular) diffusion in regions with low-moderate iron (hippocampus, caudate) and to all diffusion metrics in regions with moderate-high iron (putamen, globus pallidus). This pattern is consistent with different iron-related gliosis stages, ranging from astrogliosis that may influence intracellular diffusion in low iron regions to microglial proliferation and increased vascular permeability that may influence all sources of diffusion in high iron regions. Further, hippocampal restricted diffusion was found to be significantly related to memory performance, with a third of this effect shared with iron content; consistent with the hypothesis that higher iron-related astrogliosis in the hippocampus is associated with poorer memory performance. These results demonstrate the sensitivity of MRI to iron-related gliosis and extends our understanding of its impact on cognition by showing that these relationships also explain individual differences in memory performance.

Introduction

While the neurobiological basis of individual and age-related differences in cognition are likely multi-faceted, iron accumulation and gliosis within gray matter are recognized here as two important contributors. Rather than being independent processes, however, evidence suggests that age-related accumulation of intracellular unbound, non-heme iron (Hallgren & Sourander, 1958; Mackenzie, Iwasaki, & Tsuji, 2008; Zecca, Youdim, Riederer, Connor, & Crichton, 2004) can promote activation and proliferation of glia (gliosis; Beach, Walker, & McGeer, 1989). For example, *in vitro* (Macco et al., 2013; Pelizzoni, Zacchetti, Campanella, Grohovaz, & Codazzi, 2013) and *in vivo* (Thomsen et al., 2015; You et al., 2017) studies in animal models have directly linked iron-related inflammation to gliosis and subsequent cognitive decline, and more specifically, memory decline (Schröder, Figueiredo, & De Lima, 2013b; M. Weber et al., 2015). The recently proposed Free-Radical-Induced Energetic and Neural Decline in Senescence (FRIENDS; Raz & Daugherty, 2018) model extends these findings to human cognitive aging and suggests that magnetic resonance imaging (MRI) methods may be sensitive markers for iron-related gliosis *in vivo* for the study of cognitive aging. The current study aims to apply this model by characterizing the relationships between iron content, gray matter gliosis and memory performance using a combination of quantitative relaxometry and diffusion MRI in young and older adults who also completed a recall memory task.

While non-heme iron is essential to neurons and glia for key metabolic functions (e.g. adenosine triphosphate production, neurotransmitter synthesis; Zecca et al., 2004),

chronic iron related oxidative damage can overwhelm endogenous antioxidant defenses (e.g. glutathione; Vilhardt, Haslund-Vinding, Jaquet, & McBean, 2017) and result in reactive gliosis (Freitas, Ferreira, Trevenzoli, Oliveira, & Reis, 2017; Zecca et al., 2004). This can occur when large concentrations of intracellular iron outside binding complexes (e.g. ferritin; Connor, Menzies, Martin, & Mufson, 1990) produce reactive oxygen species by increasing pro-inflammatory cytokine expression (Macco et al., 2013; Mills et al., 2010), that directly stimulate gliosis (Burda & Sofroniew, 2014). Consistent with the FRIENDS model, the iron-related oxidative damage and subsequent gliosis drive the cumulative and progressive cognitive declines that are typical in aging. The current study will leverage individual differences in brain measures and performance between young and older adults to characterize the nature of the relationship between iron content and gliosis and their joint contributions to cognitive performance, which has not yet been assessed in humans *in vivo*.

A well-established MRI approach for measuring iron content is R_2^* relaxometry (Langkammer et al., 2010). This approach has been used in humans to demonstrate age-related accumulation of iron in the basal ganglia and hippocampus (Daugherty, Haacke, & Raz, 2015; Ghadery et al., 2015), consistent with human histological studies (Bartzokis et al., 2007; Zecca et al., 2004). Within the basal ganglia, the globus pallidus has the highest iron concentration across the adult lifespan, whereas the putamen and caudate have a moderate concentration in young adulthood and continue to accumulate iron into old age. This contrasts with the hippocampus, which has less iron concentration in young adulthood and modest accumulation with age (Ghadery et al., 2015). The current study

will leverage these regional and age group differences in iron content to characterize the relationship between iron and gliosis.

Gliosis can have several phenotypes within gray matter, including activation (e.g. astrocyte swelling; Norenberg, 1994; Pekny & Nilsson, 2005; Singh, Trivedi, Devi, Tripathi, & Khushu, 2016), proliferation (e.g. microglia recruitment; Yi et al., 2019) and dysfunction (e.g. increased blood-brain permeability; Oakley & Tharakan, 2014; Simon & Iliff, 2016). The sensitivity of diffusion imaging to gliosis phenotypes has been validated in animal models of age and acute injury (Badaut et al., 2011; Budde, Janes, Gold, Turtzo, & Frank, 2011; Debacker et al., 2020; Singh et al., 2016; R. A. Weber et al., 2017; Yi et al., 2019; Zhuo et al., 2012) and *in vitro* human (Grussu et al., 2017) studies using a combination of diffusion imaging and histology. Since diffusion imaging is sensitive to different phenotypes of gliosis, it may be used to capture different stages of gliosis (or phases, as outlined in Burda & Sofroniew, 2014, Sofroniew, 2015), seen as an increasing number of phenotypes in gray matter. Whereas most of the previous studies have used traditional single-tensor diffusion imaging to investigate gray matter gliosis, the current study will use a multicompartment diffusion approach (Neurite Orientation Dispersion and Density Imaging, NODDI; Zhang, Schneider, Wheeler-Kingshott, & Alexander, 2012), which may be more sensitive to gliosis and its differences stages across gray matter regions.

Using the framework of iron-related gliosis, NODDI and R_2^* measures can be used together to characterize the relationships between iron content and tissue microstructure. NODDI models diffusion as three primary compartments including

restricted (e.g., intracellular), hindered (e.g., extracellular), and free (e.g., cerebral spinal fluid, CSF) diffusion (Zhang et al., 2012, Fukutomi et al., 2018; Kaden, Kelm, Carson, Does, & Alexander, 2016; Rae et al., 2017). When viewed from the perspective of the iron-related gliosis, correlations between R_2^* and NODDI measures across gray matter regions can demonstrate the sensitivity of MRI techniques to regional differences in gliosis staging. For example, regions with less iron (e.g. hippocampus) are expected to display the early stages of gliosis, including astrocyte swelling (Norenberg, 1994), seen as increases in restricted diffusion. In contrast, regions with more iron (e.g. globus pallidus) may also display gliosis associated with microglia proliferation (Yi et al., 2019) and dysregulation of the blood-brain barrier (Andersen, Johnsen, & Moos, 2014), which can be seen as increases in hindered and free diffusion. Alternatively, regions with the largest age group differences in iron content (e.g., putamen) may display the most pronounced gliosis compared regions with smaller age group differences in iron (e.g., hippocampus). In either scenario, the hippocampus is likely to have relatively low levels of gliosis, however given the critical role of this region in memory performance (Lister & Barnes, 2009) even low levels of iron related gliosis can impact cognition in young and older adults.

The FRIENDS model of cognitive aging predicts a specific, but as yet untested, combined effect of iron-related gliosis on cognition. Previous studies have separately demonstrated that hippocampal iron content (Ghadery et al., 2015; Rodrigue, Daugherty, Haacke, & Raz, 2013; Schröder et al., 2013a) and microstructure (Carlesimo et al., 2010; Den Heijer et al., 2012; Radhakrishnan et al., 2020) relate to recall memory performance

measured by the Rey Auditory Verbal Learning Test (RAVLT; Saury & Emanuelson, 2017). Here, we aim to assess the combined influence of hippocampal iron and diffusion to differences in memory performance using a commonality analysis between R_2^* and NODDI measures.

Building on previous animal research and the FRIENDS model of cognitive aging, the current study aimed to characterize relationships among iron (R_2*), microstructure (hindered, restricted, free diffusion) and memory performance (RAVLT delayed) in humans using a multimodal MRI approach. The primary objectives were to: (1) replicate regional and age group differences in iron content, microstructure and memory performance; (2) examine relationships between iron and microstructure in light of the regional and age group differences in iron, and (3) test functional relevance of the iron-microstructure relationship in the hippocampus by examining their contribution to memory performance. Results are expected to show that higher iron concentration (regional difference) and accumulation (age group difference) relates to higher diffusion across the hippocampus and basal ganglia nuclei, with hippocampal iron and microstructure explaining memory performance. Consistent with the FRIENDS model, these results would provide support to the notion that human MRI data can be interpreted using mechanistic hypotheses from the animal research to ultimately better understand cognitive aging.

Materials and Methods

Participants

Young and older adults were recruited from the University of California, Riverside (UCR) and surrounding neighborhoods. Prior to enrollment, participants were screened over the phone for neurological conditions (e.g., depression, stroke), scanner related contraindications (e.g., claustrophobia, pregnancy), and general cognition using non-visual portions of the Montreal Cognitive Assessment (MoCA; Nasreddine et al., 2005; Pendlebury et al., 2017). After completing remaining portions of the MoCA in person, all participants exhibited normal cognition with scores > 23 (27.3 ± 1.63). One young and two older participants were excluded due to excessive motion in R_2* maps. The final sample included 35 young (21.06 ± 2.18 years old, 24 female) and 28 older adults (72.58 ± 6.47 years old, 13 female).

All individuals provided informed consent prior to participation in this study. The UCR Institutional Review Board approved the experimental procedures and participants were compensated for their time.

Episodic Memory Test

The Rey Auditory Verbal Learning Test (RAVLT; Rey, 1941) was administered to assess delayed free recall, measured as the number of items (out of 15) correctly recalled 30 minutes after completing five immediate free recall trials of the same word list and one immediate free recall trial of a second word list.

MRI Scanning Protocol

Imaging data were acquired using a 3T Siemens Prisma MRI (Siemens Healthineers, Malvern, PA) scanner fitted with a 32-channel receive-only head coil at the UCR Center for Advanced Neuroimaging.

A high-resolution magnetization-prepared rapid gradient-echo (MP-RAGE) image was acquired with the following parameters: echo time (TE)/repetition time (TR) = 2.72/2400 ms, 208 axial slices, voxel size = 0.8×0.8×0.8 mm, and GRAPPA acceleration factor = 2.

Two diffusion-weighted echo-planar imaging (EPI) sequences were acquired with phase-encoding directions of opposite polarity for correction of susceptibility distortions (Andersson, Skare, & Ashburner, 2003), each with the following parameters: TE/TR = 102/3500 ms, FOV = 212×182 mm, matrix size of 128×110, voxel size = 1.7×1.7×1.7 mm, 64 axial slices, and multiband acceleration factor = 4. For each acquisition, bipolar diffusion encoding gradients (b = 1500 and 3000 s/mm^2) were applied in 64 orthogonal directions, with six images having no diffusion weighting (b = 0; 12 total).

Multi-echo data derived from a 12-echo 3D gradient recalled echo (GRE) sequence were acquired with the following parameters: TE/ΔTE/TR = 4/3/40 ms, FOV = 192×224 mm, matrix size = 192×224×96, slice thickness = 1.7 mm, and GRAPPA acceleration factor = 2. Magnitude and phase images were saved for later calculation of R_2* values.

Region of Interest Segmentations

Bilateral hippocampus, caudate, putamen, and globus pallidus were automatically segmented on each participant's MP-RAGE image using FMRIB Software Library's (FSL; Jenkinson, Beckmann, Behrens, Woolrich, & Smith, 2012) Integrated Registration and Segmentation Tool (FIRST; Patenaude, Smith, Kennedy, & Jenkinson, 2011), with the flag for three-stage affine registration for hippocampus (as in Venkatesh et al., 2020). After visual inspection of each region of interest (ROI), caudate segmentations that underestimated the structure were corrected using a flag to increase the number of modes of variation for fitting from the default (40) to the maximum (336; n = 4 young) and those that were misaligned were corrected using a linear registration between the MP-RAGE and standard brain (Montreal Neurological Institute; MNI) instead of the default subcortical mask (n = 1 young). No corrections were needed for the hippocampus, putamen or globus pallidus segmentations.

Iron Image Processing

For each participant, iron data were pre-processed using the procedure outlined in Langley et al. (2019). Briefly, R_2* values were estimated using a custom script in MATLAB which fit a monoexponential model, ($S_i = S_0 \exp[-R_2 * \mathrm{TE}]$, where S_i indicates the signal of a voxel at the *i*th echo time and S_0 indicates a fitting constant) to the GRE images.

FSL's FMRIB Linear Image Registration Tool (FLIRT) was used to align the resulting R_2* map to the MPRAGE image via the magnitude image from the first echo, using a rigid body transformation (six degrees of freedom, DOF). An affine

transformation (12 DOF) with nearest neighbor interpolation was used to align the FIRST segmented ROIs into iron space using FLIRT and the matrix file from the previous step. Each bilateral iron space-aligned ROI mask was then multiplied by the voxel-wise R_2* map before taking the average across voxels and mean R_2* was extracted for each participant,

For each bilateral ROI, mean R_2* ($Iron_{raw}$) was adjusted for ROI volume using the normalization method from Jack et al. (1989). The FIRST-segmented ROI volumes ($Volume_{indiv}$) were used to calculate adjusted R_2* ($Iron_{norm}$) separately for each participant using the following equation: $Iron_{norm} = Iron_{raw} - \beta (Volume_{indiv} - Volume_{mean})$. Mean volume ($Volume_{mean}$) and slope ($\beta$) were calculated within the young adults. Volume-adjusted R_2* values were used for all analyses.

Diffusion Data Processing

For each participant, diffusion data were pre-processed using FSL, except that a binary brain mask was created using Analysis of Functional Neuro Images (AFNI; Cox 1996). After generating a field map using Topup, Eddy was used to correct for distortions due to motion, eddy-currents, and susceptibility (Andersson et al., 2003; Andersson & Sotiropoulos, 2016).

The NODDI MATLAB toolbox was then used to estimate voxel-wise measures of restricted (also known as intracellular volume fraction, ICVF), hindered (also known as orientation dispersion index, ODI) and free (also known as isotropic fraction, fISO) diffusion (http://mig.cs.ucl.ac.uk/index.php; Zhang, Schneider, Wheeler-Kingshott, & Alexander, 2012). To more accurately model diffusion within gray matter, the intrinsic

diffusivity assumption, used to estimate restricted and hindered diffusion, was set to 1.1×10^{-3} mm^2/s (Guerrero et al. 2019, Fukutomi et al., 2019, 2018).

For each participant, diffusion metrics were extracted separately for each FIRST segmented ROI. A rigid body transformation was used to align the FIRST segmented ROIs to diffusion space using FLIRT. For free diffusion, a bilateral diffusion space-aligned ROI mask was multiplied by the voxel-wise free diffusion image before taking the average across voxels. To limit hindered and restricted diffusion metrics to voxels with sufficient tissue content, an inclusion mask was created by thresholding the free diffusion image to voxels with high tissue content (free diffusion < 90%). The inclusion mask was then multiplied by each bilateral diffusion space-aligned ROI mask and then by the corresponding voxel-wise diffusion image before taking the average across voxels and hemispheres.

Statistical Analyses

Repeated measures ANOVAs (main effects; M ± SD, interactions; M ± SEM), *t*-tests and regression analyses were conducted using SPSS (Version 24.0; IBM, Armonk, NY, USA). For all analyses, the significance threshold was set to $p < 0.05$, unless otherwise noted.

To test for neural correlates of the memory measure, it is equally important to consider the correlated effect of iron content and gliosis as well as their unique effects. To determine the shared effect, a commonality analysis was performed (Lindenberger, von Oertzen, Ghisletta, & Hertzog, 2011). The commonality analysis uses a series of linear regressions to calculate the shared and unique effects of each predictor (iron

content and diffusion) and estimates the shared variance of the predictors as a proportion of the total variance explained in memory performance (shared over simple effect; SOS). Large values would indicate high commonality between predictors, which is consistent with the iron-gliosis model reviewed.

Results

Iron Content

An Age Group (young, older) × Region (hippocampus, caudate, putamen, globus pallidus) repeated measures ANOVA was conducted for R_2* (Figure 1). There was a significant effect of Region, $F(3, 183) = 492.36$, $p < 0.001$, with the highest iron content in the globus pallidus (33.46 ± 4.72), followed by the putamen (24.27 ± 4.84), caudate (20.97± 2.57), and hippocampus (16.40 ± 1.49). Post hoc pairwise comparisons revealed that iron content was significantly different between all regions, ps < 0.001.

There were also significant effects of Age Group, $F(1, 61) = 51.47$, $p < 0.001$, and Age Group × Region, $F(3, 183) = 16.77$, $p < 0.001$. Overall, iron content was higher in older adults (25.81 ± 0.38) compared to young (22.15 ± 0.34). Post hoc 2 Age Group × 2 Region comparisons revealed that the age group difference was significantly larger in the putamen (7.29 ± 0.81) compared to the caudate (3.46 ± 0.49), $F(1, 61) = 40.10$, $p < 0.001$, globus pallidum (3.06 ± 1.14), $F(1, 61) = 13.67$, $p < 0.001$, and hippocampus (0.83 ± 0.37), $F(1, 61) = 49.27$, $p < 0.001$; and in the caudate compared to the hippocampus, $F(1, 61) = 49.27$, $p < 0.001$. The age-related differences in globus pallidus were statistically equivalent to that in the caudate ($p > 0.20$) and hippocampus ($p > 0.05$).

Microstructure

Age Group (young, older) × Region (hippocampus, caudate, putamen, globus pallidus) repeated measures ANOVAs were conducted separately for each diffusion metric. In the event of significant interactions, post-hoc Age Group × Region ANOVAs for each pair of regions was conducted.

Restricted Diffusion

There was a significant effect of Region, $F(3, 183) = 1851.3$, $p < 0.001$, with the highest restricted diffusion in the globus pallidus (0.89 ± 0.06), followed by the putamen (0.50 ± 0.12), caudate (0.43 ± 0.07), and hippocampus (0.41 ± 0.05). Post hoc pairwise comparisons revealed that restricted diffusion was significantly different between all regions, ps < 0.008.

There were significant effects of Age Group, $F(1, 61) = 102.84$, $p < 0.001$, and Age Group × Region, $F(3, 183) = 41.05$, $p < 0.001$. Overall, restricted diffusion was higher in older adults (0.61 ± 0.01) compared to young (0.51 ± 0.01). Post hoc 2 Age Group × 2 Region comparisons for each combination of regions revealed that the age group difference was significantly larger in the putamen (0.19 ± 0.02) compared to the caudate (0.11 ± 0.01), $F(1, 61) = 46.97$, $p < 0.001$, globus pallidus (0.06 ± 0.01), $F(1, 61) = 78.73$, $p < 0.001$, and hippocampus (0.05 ± 0.01), $F(1, 61) = 65.11$, $p < 0.001$; in the caudate compared to the globus pallidus (0.05 ± 0.01), $F(1, 61) = 14.95$, $p < 0.001$, and hippocampus, $F(1, 61) = 20.76$, $p < 0.01$; and in the globus pallidus compared to the hippocampus, $F(1, 61) = 0.09$, $p < 0.001$.

Hindered Diffusion

The effect of Region was not significant, $p > 0.08$, but there were significant effects of Age Group, $F(1, 61) = 16.10$, $p < 0.001$, and Age Group × Region, $F(3, 183) = 21.63$, $p < 0.001$. Hindered diffusion was higher in older adults (0.42 ± 0.01) compared to young (0.40 ± 0.01). Post hoc 2 Age Group × 2 Region comparisons revealed that the age group difference was significantly larger in the hippocampus (0.06 ± 0.01) compared to the caudate, $F(1, 61) = 74.63$, $p < 0.001$, putamen, $F(1, 61) = 58.46$, $p < 0.001$, and globus pallidus, $F(1, 61) = 19.84$, $p < 0.001$. The results did not statistically differ between the remaining regions, ps > 0.09.

Free Diffusion

There was a significant effect of Region, $F(3, 183) = 81.37$, $p < 0.001$, with the highest free diffusion in the hippocampus (0.30 ± 0.04), followed by globus pallidus (0.29 ± 0.05), caudate (0.23 ± 0.07) and putamen (0.20 ± 0.08). Post hoc pairwise comparisons revealed that free diffusion was significantly different between all regions, ps < 0.001. The results did not statistically differ between globus pallidus and hippocampus, $p > 0.23$.

There were also significant effects of Age Group, $F(1, 61) = 58.14$, $p < 0.001$, and Age Group × Region, $F(3, 183) = 34.22$, $p < 0.001$. Overall, free diffusion was higher in older (0.29 ± 0.01) compared to young (0.22 ± 0.01) adults. Post hoc 2 Age Group × 2 Region comparisons revealed that the age group difference was significantly larger in the hippocampus (0.05 ± 0.02) compared to the globus pallidus (0.01 ± 0.01), $F(1, 61) = 9.66$, $p < 0.004$, caudate (0.11 ± 0.04), $F(1, 61) = 31.74$, $p < 0.001$, and putamen (0.12 ±

0.03), $F(1, 61) = 61.00$, $p < 0.001$; and in the globus pallidus compared to the caudate, $F(1, 61) = 40.81$, $p < 0.001$, and putamen, $F(1, 61) = 58.92$, $p < 0.001$. The results did not statistically differ between the remaining regions, ps > 0.30.

Relation between Iron and Microstructure

Separate linear regressions for each region tested the relationship between iron content (R_2*) and each diffusion metric, as well as the potential moderating effect of age group (by including Age Group × R_2* as a predictor). Age group was included as a covariate given the previously described age effects. Significant effects were Bonferroni corrected for three comparisons per diffusion metric ($p < 0.02$; Figure 2). Age group was included as a covariate in all models.

For the hippocampus, ß = 0.34, $t(62) = 3.31$, $p < 0.003$, and caudate, ß = 0.39, $t(62) = 3.75$, $p < 0.001$, significant positive relationships were observed between R_2* and restricted diffusion, but not hindered or free diffusion, ps > 0.03. For the putamen, significant positive relationships were observed between R_2* and restricted, ß = 0.67, $t(62) = 8.85$, $p < 0.001$, hindered, ß = 0.95, $t(62) = 6.23$, $p < 0.001$, and free, ß = 0.54, $t(62) = 4.98$, $p < 0.001$, diffusion. For the globus pallidus, significant positive relationships were observed between R_2* and restricted, ß = 0.40, $t(62) = 3.83$, $p < 0.001$, and hindered, ß = 0.52, $t(62) = 4.52$, $p < 0.001$, diffusion, whereas a significant negative relationship was observed between R_2* and free diffusion, ß = -0.47, $t(62) = -3.83$, $p < 0.001$. There was no evidence of age group moderating these relations in any region, ps > 0.10, indicating that the R_2*-diffusion relationship was comparable in young and older adults.

Contributions of Iron and Microstructure to Memory Performance

An independent sample *t*-test assessed age group differences in RAVLT delayed recall, $t(47) = -4.06$, $p < 0.001$, 95% CI [-4.90, -1.66]. As expected, older adults (8.04 ± 3.59) recalled significantly fewer words than young (11.31 ± 2.57).

A commonality analysis quantified the shared variance between hippocampal iron (R_2*) and microstructure (restricted diffusion) in explaining in memory performance (delayed free recall). These analyses were limited to the hippocampus due to its known role in memory and to the restricted diffusion metric given its previously described relationship to hippocampal iron. Results revealed that 31.5%, $R^2 = 0.32$, $p < 0.001$, of the variance in delayed recall performance was explained by restricted diffusion alone, 11.8% by R_2* alone, and a total of 32.4% when both restricted diffusion and R_2* were included in the model (see Table 1). From this procedure, of the total variance in RAVLT recall that was explained by diffusion, 34.6% of the effect was shared with hippocampal R_2*.

Since the variance in delayed recall performance explained by our metrics of interest may be shared with age, the commonality analysis was repeated after including age group as a covariate (see Figure 3). In this model, restricted diffusion uniquely explained 12.7% of variance in delayed recall, $R^2 = 0.13$, $p < 0.001$, the unique effect of R_2* was 4.8%, $R^2 = 0.05$, $p = 0.05$, and the total effect of both predictors was 13.5%. Therefore, even independent of age group, 31.5% of the total variance in delayed recall that was explained by hippocampal restricted diffusion was shared with hippocampal R_2*. Taken together, hippocampus microstructure significantly contributes to memory

performance independent of age, and approximately 32% of its effect is also related to iron content.

Discussion

The current study tested the relationships between iron, gliosis, and memory in humans using a combination of neuroimaging techniques, consistent with the FRIENDS model of cognitive aging. Our results revealed several major findings. First, we replicated well-known regional and age group differences in iron content (R_2*), tissue microstructure (NODDI) and memory performance (RAVLT delayed recall). Second, we observed relationships between iron and microstructure that were specific to restricted diffusion in the hippocampus and caudate, whereas significant relationships were observed in all diffusion measures in the putamen and globus pallidus, consistent with stages of gliosis as a function of regional iron content. Moreover, these iron-microstructure relationships were not moderated by age group, suggesting that the effect of iron on microstructure may be cumulative and progressive across the adult lifespan. Third, restricted diffusion in the hippocampus related to recall memory performance, with a third of this variance shared with iron. These results demonstrate that MRI is sensitive to iron-related gliosis within gray matter, which contributes to individual differences in memory performance.

Age group and regional differences in NODDI measures and iron content (R_2*), replicated previous studies (Franco et al., 2020; Ghadery et al., 2015; Nazeri et al., 2015; Venkatesh et al., 2020) and may predict relationships between iron and diffusion measures. The main effect of region revealed that globus pallidus and putamen had the

highest iron content followed by caudate and hippocampus. In contrast, the main effect of age group revealed that putamen and caudate showed the largest age group differences in iron, followed by globus pallidus and hippocampus. These results predict that differences in either regional iron or age group will be better associated with gliosis, characterized by R_2* relating to one or more NODDI metrics.

We observed significant relationships between iron content and microstructure that varied across the hippocampus and basal ganglia nuclei. Within the hippocampus and caudate, relationships between R_2*and NODDI metrics were specific to restricted diffusion. Of note, these regions had low to moderate overall iron concentration. We interpret this pattern of results as being consistent with an earlier stage of iron-related gliosis (Norenberg, 1994; Pekny & Nilsson, 2005), in which astrocyte activation and swelling are limited to the intracellular source of diffusion. The positive direction of these effects also supports the notion that higher iron content is accompanied by reactive astrogliosis through oxidative damage, and hence an increase in intracellular sources of diffusion. Proposing astrogliosis as a potential mechanism that influences restricted diffusion extends previous work that has traditionally attributed this diffusion metric to neurite density (Fukutomi et al., 2019; Grussu et al., 2017; Metzler-Baddeley et al., 2019; Radhakrishnan et al., 2020) and provides a parsimonious explanation for previous observations of age-related *increases* in gray matter restricted diffusion seen by our group (Franco et al., 2020; Venkatesh et al., 2020) among others (Metzler-Baddeley et al., 2019; Radhakrishnan et al., 2020).

In contrast, within the putamen and globus pallidus, R_2* was related to all three diffusion metrics. These regions had moderate to high overall iron concentration. This pattern of results may indicate later stages of iron-related gliosis in which astrogliosis is coupled with microglia proliferation (Yi et al., 2019) and increased vascular permeability (Elahy et al., 2015) that would influence extracellular and free, not just intracellular, sources of diffusion. Recent evidence supports the notion that hindered diffusion is sensitive to infiltrating microglia, as one study demonstated that hindered diffusion significantly varied depending on microglia density in mice (Yi et al., 2019). Whereas R_2* was only positively related to restricted and hindered diffusion, positive (putamen) and negative (globus pallidus) correlations were seen for free diffusion, which likely reflects low signal to noise ratios in the diffusion signal within the globus pallidus. Taken together, the regional patterns between iron content and microstructure observed here appear to reflect an iron concentration-dependent effect on microstructure. As such, our findings are consistent with and extend the iron-gliosis hypothesis in humans by demonstrating that increased iron accumulation in gray matter is accompanied by a glial response that can be detected initially with intracellular (restricted) and then extracellular (hindered, free) diffusion metrics. Further, by finding that the iron-microstructure relationships were comparable between young and older adults across the hippocampus and all basal ganglia nuclei, our results suggest that iron-related gliosis is cumulative and progressive across the lifespan.

Finally, we demonstrated the shared consequence of hippocampal iron-related gliosis on recall memory performance, providing functional relevance to the current

findings. Greater hippocampal restricted diffusion explained 31.5% of the variance in memory performance, 34.6% of this effect was shared with hippocampal R_2*. Consistent with our interpretation of a cumulative effect of iron across the lifespan, approximately 31.5% of shared variance between microstructure and iron estimates remained after statistically controlling for age. These findings extend at least one previous study that observed that higher restricted diffusion related to poorer memory performance in younger and older adults (Radhakrishnan et al., 2020) by revealing the extent to which this diffusion-memory relationship is shared with iron. More importantly, these behavioral results provide an important piece of evidence in support of the iron-gliosis hypothesis and FRIENDS model by demonstrating the sensitivity of MRI to iron-related hippocampal astrogliosis as a correlate to memory performance.

In conclusion, the current study revealed key pieces of evidence in support of the iron-gliosis hypothesis in humans. We found significant relationships between iron content and tissue microstructure that systematically varied across subcortical regions (but not age group) in an iron concentration-dependent manner. This has functional consequences as iron content and tissue microstructure together contribute to recall memory performance, independent of age. This study represents an important validation and extension of the animal literature that gave rise to the iron-gliosis hypothesis, that accumulation of iron in gray matter can cause gliosis through oxidative stress, and the FRIENDS model, by demonstrating that MRI is sensitive to individual differences in iron and gliosis, and that their combined effect explains memory performance.

Figure 8
Iron content (R_2*) and microstructure (restricted, hindered, free diffusion) are shown separately for young (black circles, stripe bar) and older (open circles, open bar) adults in each region of interest. *** $p < 0.001$, * = $p < 0.05$

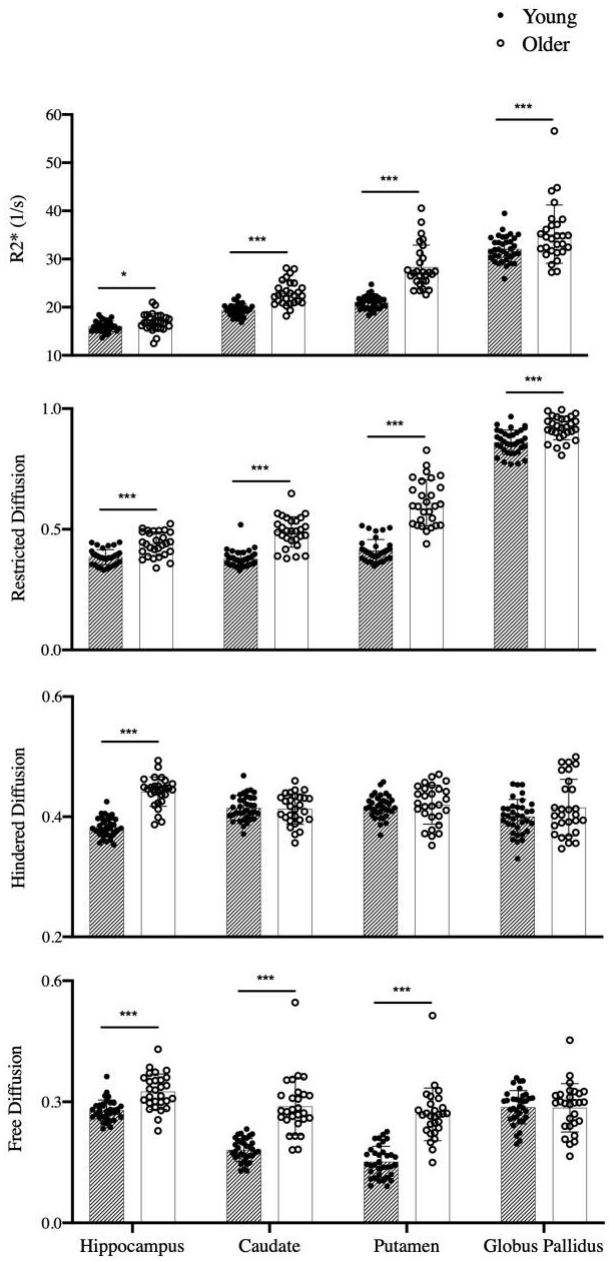

Figure 9
Significant relationships between iron content (R_2*) and microstructure (restricted, hindered, free diffusion) are shown separately for each region after controlling for age group.

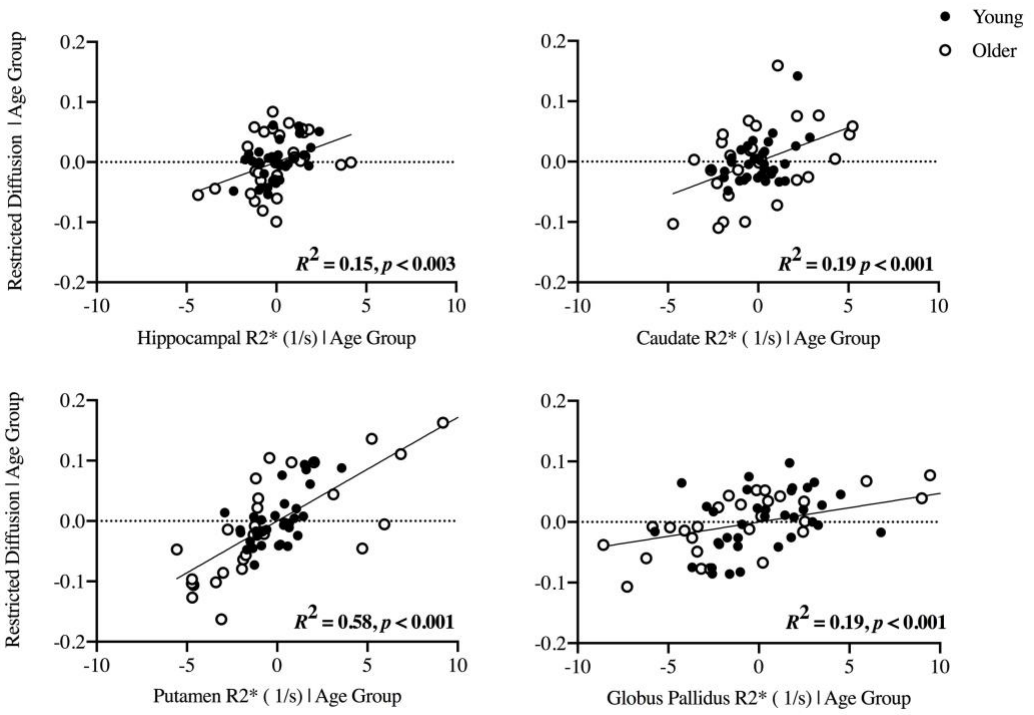

Table 6

Summary of regression models for the commonality analysis of NODDI diffusion and R_2* in the hippocampus predicting memory performance.

Model	R^2	*F*	df	*p*
Restricted Diffusion	0.32	28.10	(1, 62)	.000
R2*	0.12	8.17	(1, 62)	.006
Total Effect of Restricted and R2*	0.32	14.36	(2,62)	.000

Dependent Variable: RAVLT delayed recall.

df = degrees of freedom (regression, total)

Figure 10
Associations between hippocampal restricted diffusion and RAVLT delayed recall performance, collapsed across age groups.

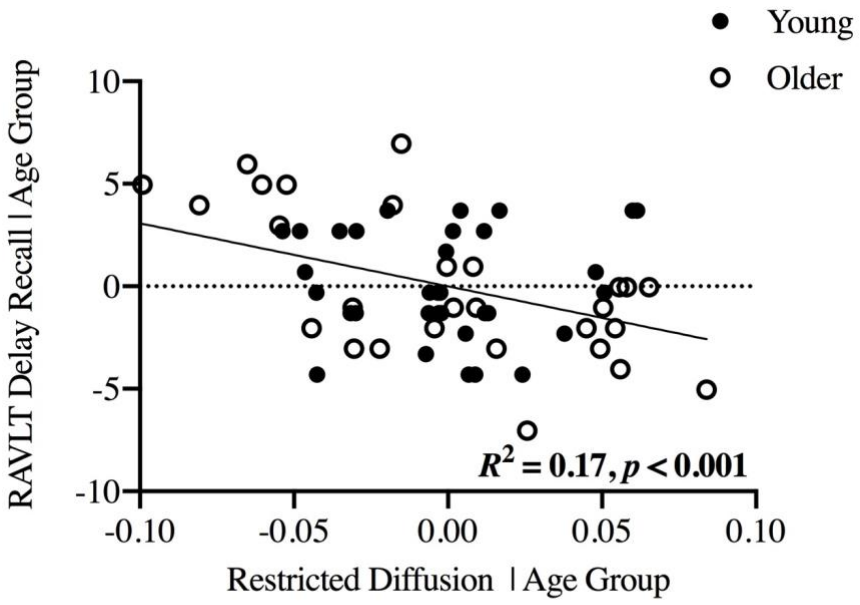

References

Andersen, H. H., Johnsen, K. B., & Moos, T. (2014, November 12). Iron deposits in the chronically inflamed central nervous system and contributes to neurodegeneration. *Cellular and Molecular Life Sciences*. Birkhauser Verlag AG. https://doi.org/10.1007/s00018-013-1509-8

Andersson, J. L. R., Skare, S., & Ashburner, J. (2003). How to correct susceptibility distortions in spin-echo echo-planar images: application to diffusion tensor imaging. *NeuroImage*, *20*(2), 870–888. https://doi.org/10.1016/S1053-8119(03)00336-7

Andersson, J. L. R., & Sotiropoulos, S. N. (2016). An integrated approach to correction for off-resonance effects and subject movement in diffusion MR imaging. *Neuroimage*, *125*, 1063. https://doi.org/10.1016/J.NEUROIMAGE.2015.10.019

Badaut, J., Ashwal, S., Adami, A., Tone, B., Recker, R., Spagnoli, D., … Obenaus, A. (2011). Brain water mobility decreases after astrocytic aquaporin-4 inhibition using RNA interference. *Journal of Cerebral Blood Flow and Metabolism : Official Journal of the International Society of Cerebral Blood Flow and Metabolism*, *31*(3), 819–831. https://doi.org/10.1038/jcbfm.2010.163

Bartzokis, G., Tishler, T. A., Lu, P. H., Villablanca, P., Altshuler, L. L., Carter, M., … Mintz, J. (2007). Brain ferritin iron may influence age- and gender-related risks of neurodegeneration. *Neurobiology of Aging*, *28*(3), 414–423. https://doi.org/10.1016/j.neurobiolaging.2006.02.005

Beach, T. G., Walker, R., & McGeer, E. G. (1989). Patterns of gliosis in alzheimer's disease and aging cerebrum. *Glia*, *2*(6), 420–436. https://doi.org/10.1002/glia.440020605

Bennett, I. J., Huffman, D. J., & Stark, C. E. L. (2015). Limbic tract integrity contributes to pattern separation performance across the lifespan. *Cerebral Cortex*, *25*(9), 2988–2999. https://doi.org/10.1093/cercor/bhu093

Budde, M. D., Janes, L., Gold, E., Turtzo, L. C., & Frank, J. A. (2011). The contribution of gliosis to diffusion tensor anisotropy and tractography following traumatic brain injury: Validation in the rat using Fourier analysis of stained tissue sections. *Brain*, *134*(8), 2248–2260. https://doi.org/10.1093/brain/awr161

Burda, J. E., & Sofroniew, M. V. (2014, January 22). Reactive gliosis and the multicellular response to CNS damage and disease. *Neuron*. NIH Public Access. https://doi.org/10.1016/j.neuron.2013.12.034

Carlesimo, G. A., Cherubini, A., Caltagirone, C., & Spalletta, G. (2010). Hippocampal mean diffusivity and memory in healthy elderly individuals: A cross-sectional study. *Neurology*, *74*(3), 194–200. https://doi.org/10.1212/WNL.0b013e3181cb3e39

Connor, J. R., Menzies, S. L., Martin, S. M. S., & Mufson, E. J. (1990). Cellular distribution of transferrin, ferritin, and iron in normal and aged human brains. *Journal of Neuroscience Research*, *27*(4), 595–611. https://doi.org/10.1002/jnr.490270421

Daugherty, A. M., Haacke, X. E. M., & Raz, N. (2015). Striatal Iron Content Predicts Its Shrinkage and Changes in Verbal Working Memory after Two Years in Healthy Adults. https://doi.org/10.1523/JNEUROSCI.4717-14.2015

Debacker, C., Djemai, B., Ciobanu, L., Tsurugizawa, T., & Bihan, D. Le. (2020). Diffusion MRI reveals in vivo and non-invasively changes in astrocyte function induced by an aquaporin-4 inhibitor. *PLoS ONE*, *15*(5). https://doi.org/10.1371/journal.pone.0229702

Den Heijer, T., der Lijn, F. van, Vernooij, M. W., de Groot, M., Koudstaal, P. J., der Lugt, A. van, … Breteler, M. M. B. (2012). Structural and diffusion MRI measures of the hippocampus and memory performance. *NeuroImage*, *63*(4), 1782–1789. https://doi.org/10.1016/j.neuroimage.2012.08.067

Elahy, M., Jackaman, C., Mamo, J. C., Lam, V., Dhaliwal, S. S., Giles, C., … Takechi, R. (2015). Blood-brain barrier dysfunction developed during normal aging is associated with inflammation and loss of tight junctions but not with leukocyte recruitment. *Immunity & Ageing : I & A*, *12*, 2. https://doi.org/10.1186/s12979-015-0029-9

Franco, C. Y., Petok, J. R., Langley, J., Hu, X., & Bennett, I. J. (2020). Implicit associative learning relates to basal ganglia gray matter microstructure in young and older adults. *Behavioural Brain Research*, *397*. https://doi.org/10.1016/j.bbr.2020.112950

Freitas, H. R., Ferreira, G. D. C., Trevenzoli, I. H., Oliveira, K. D. J., & Reis, R. A. D. M. (2017, November 20). Fatty acids, antioxidants and physical activity in brain aging. *Nutrients*. MDPI AG. https://doi.org/10.3390/nu9111263

Fukutomi, H., Glasser, M. F., Murata, K., Akasaka, T., Fujimoto, K., Yamamoto, T., … Hayashi, T. (2019). Diffusion Tensor Model links to Neurite Orientation Dispersion and Density Imaging at high b-value in Cerebral Cortical Gray Matter. *Scientific Reports*, *9*(1), 12246. https://doi.org/10.1038/s41598-019-48671-7

Fukutomi, H., Glasser, M. F., Zhang, H., Autio, J. A., Coalson, T. S., Okada, T., … Hayashi, T. (2018). Neurite imaging reveals microstructural variations in human

cerebral cortical gray matter. *NeuroImage*, *182*, 488–499. https://doi.org/10.1016/J.NEUROIMAGE.2018.02.017

Ghadery, C., Pirpamer, L., Hofer, E., Langkammer, C., Petrovic, K., Loitfelder, M., … Schmidt, R. (2015). R2* mapping for brain iron: Associations with cognition in normal aging. *Neurobiology of Aging*, *36*(2), 925–932. https://doi.org/10.1016/j.neurobiolaging.2014.09.013

Grussu, F., Schneider, T., Tur, C., Yates, R. L., Tachrount, M., Ianuş, A., … Gandini Wheeler-Kingshott, C. A. M. (2017). Neurite dispersion: a new marker of multiple sclerosis spinal cord pathology? *Annals of Clinical and Translational Neurology*, *4*(9), 663–679. https://doi.org/10.1002/acn3.445

Guerrero, J. M., Adluru, N., Bendlin, B. B., Goldsmith, H. H., Schaefer, S. M., Davidson, R. J., … Alexander, A. L. (2019). Optimizing the intrinsic parallel diffusivity in NODDI: An extensive empirical evaluation. *PLOS ONE*, *14*(9), e0217118. https://doi.org/10.1371/journal.pone.0217118

Hallgren, B., & Sourander, P. (1958). THE EFFECT OF AGE ON THE NON-HAEMIN IRON IN THE HUMAN BRAIN. *Journal of Neurochemistry*, *3*(1), 41–51. https://doi.org/10.1111/j.1471-4159.1958.tb12607.x

Jenkinson, M., Beckmann, C. F., Behrens, T. E. J., Woolrich, M. W., & Smith, S. M. (2012). FSL. *NeuroImage*, *62*(2), 782–790. https://doi.org/10.1016/J.NEUROIMAGE.2011.09.015

Keuken, M. C., Bazin, P. L., Backhouse, K., Beekhuizen, S., Himmer, L., Kandola, A., … Forstmann, B. U. (2017). Effects of aging on T1 , T2∗ , and QSM MRI values in the subcortex. *Brain Structure and Function*, *222*(6), 2487–2505. https://doi.org/10.1007/s00429-016-1352-4

Langkammer, C., Krebs, N., Goessler, W., Scheurer, E., Ebner, F., Yen, K., … Ropele, S. (2010). Quantitative MR imaging of brain iron: A postmortem validation study. *Radiology*, *257*(2), 455–462. https://doi.org/10.1148/radiol.10100495

Lindenberger, U., von Oertzen, T., Ghisletta, P., & Hertzog, C. (2011). Cross-Sectional Age Variance Extraction: What's Change Got To Do With It? *Psychology and Aging*, *26*(1), 34–47. https://doi.org/10.1037/a0020525

Lister, J. P., & Barnes, C. A. (2009). Neurobiological changes in the hippocampus during normative aging. *Archives of Neurology*, *66*(7), 829–833. https://doi.org/10.1001/archneurol.2009.125

Macco, R., Pelizzoni, I., Consonni, A., Vitali, I., Giacalone, G., Martinelli Boneschi, F., … Zacchetti, D. (2013). Astrocytes acquire resistance to iron-dependent oxidative stress upon proinflammatory activation. *Journal of Neuroinflammation*, *10*(1), 897. https://doi.org/10.1186/1742-2094-10-130

Mackenzie, E. L., Iwasaki, K., & Tsuji, Y. (2008, June 1). Intracellular iron transport and storage: From molecular mechanisms to health implications. *Antioxidants and Redox Signaling*. Antioxid Redox Signal. https://doi.org/10.1089/ars.2007.1893

Metzler-Baddeley, C., Mole, J. P., Sims, R., Fasano, F., Evans, J., Jones, D. K., … Baddeley, R. J. (2019). Fornix white matter glia damage causes hippocampal gray matter damage during age-dependent limbic decline. *Scientific Reports*, *9*(1). https://doi.org/10.1038/s41598-018-37658-5

Mills, E., Dong, X. P., Wang, F., & Xu, H. (2010, January). Mechanisms of brain iron transport: Insight into neurodegeneration and CNS disorders. *Future Medicinal Chemistry*. NIH Public Access. https://doi.org/10.4155/fmc.09.140

Nasreddine, Z. S., Phillips, N. A., BÃ©dirian, V., Charbonneau, S., Whitehead, V., Collin, I., … Chertkow, H. (2005). The Montreal Cognitive Assessment, MoCA: A Brief Screening Tool For Mild Cognitive Impairment. *Journal of the American Geriatrics Society*, *53*(4), 695–699. https://doi.org/10.1111/j.1532-5415.2005.53221.x

Nazeri, A., Chakravart, M., Rotenberg, D. J., Rajji, T. K., Rathi, X., Michailovich, O. V., & Voineskos, A. N. (2015). Functional consequences of neurite orientation dispersion and density in humans across the adult lifespan. *Journal of Neuroscience*, *35*(4), 1753–1762. https://doi.org/10.1523/JNEUROSCI.3979-14.2015

Norenberg, M. D. (1994). Astrocyte Responses to CNS Injury. *Journal of Neuropathology and Experimental Neurology*, *53*(3), 213–220. https://doi.org/10.1097/00005072-199405000-00001

Oakley, R., & Tharakan, B. (2014). Vascular Hyperpermeability and Aging. *Aging and Disease*, *5*(2), 114–125. https://doi.org/10.14336/AD.2014.0500114

Pekny, M., & Nilsson, M. (2005). Astrocyte activation and reactive gliosis. *Glia*, *50*(4), 427–434. https://doi.org/10.1002/glia.20207

Pelizzoni, I., Zacchetti, D., Campanella, A., Grohovaz, F., & Codazzi, F. (2013). Iron uptake in quiescent and inflammation-activated astrocytes: A potentially neuroprotective control of iron burden. *Biochimica et Biophysica Acta - Molecular Basis of Disease*, *1832*(8), 1326–1333. https://doi.org/10.1016/j.bbadis.2013.04.007

Pendlebury, S. T., Welch, S. J. V, Cuthbertson, F. C., Mariz, J., Mehta, Z., & Rothwell, P. M. (2017). Telephone assessment of cognition after TIA and stroke : TICSm and telephone MoCA vs face-to-face MoCA and neuropsychological battery. *Stroke*, *44*(1), 227–229. https://doi.org/10.1161/STROKEAHA.112.673384.Telephone

Radhakrishnan, H., Stark, S. M., & Stark, C. E. L. (2020). Microstructural Alterations in Hippocampal Subfields Mediate Age-Related Memory Decline in Humans. *Frontiers in Aging Neuroscience*, *12*. https://doi.org/10.3389/fnagi.2020.00094

Rey, A. (1941). L'examen psychologique dans les cas d'encéphalopathie traumatique. https://doi.org/1943-03814-001

Rodrigue, K. M., Daugherty, A. M., Haacke, E. M., & Raz, N. (2013). The role of hippocampal iron concentration and hippocampal volume in age-related differences in memory. *Cerebral Cortex*, *23*(7), 1533–1541. https://doi.org/10.1093/cercor/bhs139

Schröder, N., Figueiredo, L. S., & De Lima, M. N. M. (2013a). Role of brain iron accumulation in cognitive dysfunction: Evidence from animal models and human studies. *Journal of Alzheimer's Disease*, *34*(4), 797–812. https://doi.org/10.3233/JAD-121996

Schröder, N., Figueiredo, L. S., & De Lima, M. N. M. (2013b). Role of brain iron accumulation in cognitive dysfunction: Evidence from animal models and human studies. *Journal of Alzheimer's Disease*. IOS Press. https://doi.org/10.3233/JAD-121996

Simon, M. J., & Iliff, J. J. (2016, March 1). Regulation of cerebrospinal fluid (CSF) flow in neurodegenerative, neurovascular and neuroinflammatory disease. *Biochimica et Biophysica Acta - Molecular Basis of Disease*. Elsevier. https://doi.org/10.1016/j.bbadis.2015.10.014

Singh, K., Trivedi, R., Devi, M. M., Tripathi, R. P., & Khushu, S. (2016). Longitudinal changes in the DTI measures, anti-GFAP expression and levels of serum inflammatory cytokines following mild traumatic brain injury ☆. *Experimental Neurology*, *275*, 427–435. https://doi.org/10.1016/j.expneurol.2015.07.016

Sofroniew, M. V. (2015). Astrogliosis. *Cold Spring Harbor Perspectives in Biology*, *7*(2). https://doi.org/10.1101/cshperspect.a020420

Thomsen, M. S., Andersen, M. V., Christoffersen, P. R., Jensen, M. D., Lichota, J., & Moos, T. (2015). Neurodegeneration with inflammation is accompanied by accumulation of iron and ferritin in microglia and neurons. *Neurobiology of Disease*, *81*, 108–118. https://doi.org/10.1016/j.nbd.2015.03.013

Venkatesh, A., Stark, S. M., Stark, C. E. L., & Bennett, I. J. (2020). Age- and memory-related differences in hippocampal gray matter integrity are better captured by NODDI compared to single-tensor diffusion imaging. *Neurobiology of Aging*, *96*, 12–21. https://doi.org/10.1016/j.neurobiolaging.2020.08.004

Vilhardt, F., Haslund-Vinding, J., Jaquet, V., & McBean, G. (2017). Microglia antioxidant systems and redox signalling. *British Journal of Pharmacology*. John Wiley and Sons Inc. https://doi.org/10.1111/bph.13426

Weber, M., Wu, T., Hanson, J. E., Alam, N. M., Solanoy, H., Ngu, H., … Levie, K. S. (2015). Cognitive deficits, changes in synaptic function, and brain pathology in a mouse model of normal aging. *ENeuro*, *2*(5), 47–62. https://doi.org/10.1523/ENEURO.0047-15.2015

Weber, R. A., Chan, C. H., Nie, X., Maggioncalda, E., Valiulis, G., Lauer, A., … Adkins, D. A. L. (2017). Sensitivity of diffusion MRI to perilesional reactive astrogliosis in focal ischemia. *NMR in Biomedicine*, *30*(7). https://doi.org/10.1002/nbm.3717

Yi, S. Y., Barnett, B. R., Torres-Velázquez, M., Zhang, Y., Hurley, S. A., Rowley, P. A., … Yu, J. P. J. (2019). Detecting microglial density with quantitative multi-compartment diffusion MRI. *Frontiers in Neuroscience*. https://doi.org/10.3389/fnins.2019.00081

You, L. H., Yan, C. Z., Zheng, B. J., Ci, Y. Z., Chang, S. Y., Yu, P., … Chang, Y. Z. (2017). Astrocyte hepcidin is a key factor in LPS-induced neuronal apoptosis. *Cell Death & Disease*, *8*(3), e2676. https://doi.org/10.1038/cddis.2017.93

Zecca, L., Youdim, M. B. H., Riederer, P., Connor, J. R., & Crichton, R. R. (2004, November). Iron, brain ageing and neurodegenerative disorders. *Nature Reviews Neuroscience*. Nat Rev Neurosci. https://doi.org/10.1038/nrn1537

Zhang, H., Schneider, T., Wheeler-Kingshott, C. A., & Alexander, D. C. (2012). NODDI: Practical in vivo neurite orientation dispersion and density imaging of the human brain. *NeuroImage*, *61*(4), 1000–1016. https://doi.org/10.1016/j.neuroimage.2012.03.072

Zhuo, J., Xu, S., Proctor, J. L., Mullins, R. J., Simon, J. Z., Fiskum, G., & Gullapalli, R. P. (2012). Diffusion kurtosis as an in vivo imaging marker for reactive astrogliosis in traumatic brain injury. *NeuroImage*, *59*(1), 467–477. https://doi.org/10.1016/j.neuroimage.2011.07.050

Conclusion

Overall, the current body of work has demonstrated the value of multi-compartment diffusion imaging (NODDI) for characterizing gray matter microstructure and has identified how specific microstructural features (e.g., glia, CSF) relate to age and memory performance. The first two chapters confirmed that multi-compartment diffusion measures of restricted, hindered, and free diffusion are more sensitive to age and memory performance than DTI measures. The third chapter applied these findings to a theoretical framework of iron-related gliosis in the basal ganglia and hippocampus and tested the hypothesis that age-related increases in NODDI measures were related to increases in gray matter iron content, that were regionally dependent. All three chapters examined relationships to memory performance and identified that depending on the region, both tissue and non-tissue compartments can relate to different facets of memory. Overall, these results establish a foundation for the use NODDI in characterizing age-related differences in gray matter microstructure, while linking animal and human studies to advancing knowledge about how the brain informs cognition.

The first chapter directly compared the sensitivity of DTI and NODDI measures to age within hippocampal gray matter and assessed if these measures predicted memory performance. Thresholding DTI measures by free diffusion significantly attenuated the age group differences, and logistic regression results confirmed that free diffusion along with hindered diffusion was significantly associated with age. Results also found a moderating effect of age group on the relationship between hippocampal hindered diffusion and mnemonic discrimination, such that lower hindered diffusion was related to

better discrimination performance in young but not older adults. In sum, this chapter demonstrated that NODDI measures were more sensitive to age-related differences than DTI, likely due to its ability to more accurately model complex gray matter microstructure. While this chapter was limited to the hippocampus and relationships to mnemonic discrimination, the following chapter extended these finding to regions including cortex and basal ganglia and included measures of verbal recall and recognition to characterize additional relationships to memory performance.

Chapter two extended the comparisons between DTI and NODDI and relationships to age and memory performance to cortical lobes and basal ganglia, while also examining hippocampal gray matter. Importantly, this was the first study to comprehensively characterize brain wide gray matter microstructure and relationships to memory performance using both DTI and NODDI measures, in young and older adults. Results revealed that restricted diffusion was significantly higher in older adults compared to young in all ROIs examined, and logistic regression analysis revealed that the overall best predictor of age was frontal lobe free diffusion. Relationships to performance in the hippocampus suggest that tissue compartments are sensitive to specific facets of memory (mnemonic discrimination vs. recall memory), whereas free water is more sensitive to recall memory performance in both cortical lobes and putamen. The overall pattern of results confirms that NODDI outperforms DTI to capture age and memory performance in gray matter regions beyond hippocampus. These results emphasize the need for studies which use diffusion imaging in conjunction with other neuroimaging techniques (e.g., iron imaging, positron emission tomography) to parse out

the relative contributions of specific tissue features to the NODDI measures, since these measures likely capture the contributions of both glia and neurons.

In service of this goal, chapter three tested the relationships between iron, gliosis, and memory in humans using a combination of diffusion imaging with quantitative relaxometry, consistent with the FRIENDS model of cognitive aging. Previously observed age group differences in chapters 2 and 3 suggested that diffusion imaging was sensitive to different glial phenotypes, so relationships between iron content (R_2*) and NODDI that varied by region was largely unsurprising. Interestingly, the results did not find that iron-microstructure relationships were moderated by age group but instead were comparable between young and older adults, which suggests that the effect of iron on microstructure may be progressive across the adult lifespan. This study represents an important validation and extension of the animal model of iron-related gray matter gliosis, that both NODDI and quantitative relaxometry are sensitive to, consistent with the FRIENDS model. This chapter establishes that MRI sensitive to individual differences in iron and gliosis, and that their combined effect can explain differences in recall memory performance.

In conclusion, this body of work provides a framework for investigating relationships with gray matter microstructure, age and memory performance using a cross-sectional design in young and older adults. The results demonstrate that this approach can be used to replicate and extend existing hypotheses of cognitive aging from both human and animal studies, such as the frontal lobe hypothesis and model of iron related gliosis. Extension of patterns in the hippocampus and cortex from fMRI and

lesion studies suggest that NODDI measures have strong concordance with the rest of the aging literature and that the use of one or more MRI techniques with NODDI can improve understanding of *in vivo* brain-behavior relationships in humans. In the future, multi-compartment diffusion imaging will undoubtably be a valuable tool in developing biomarkers of age and for better understanding how memory declines with age.